CHARACTERIZATION OF DISSIPATIVE STATES IN NIOBIUM TITANIUM NITRIDE SUPERCONDUCTING FILAMENTS

BY

FATAI OLAWALE BAKARE

A Thesis Presented to the

DEANSHIP OF GRADUATE STUDIES

KING FAHD UNIVERSITY OF PETROLEUM & MINERALS

DHAHRAN, SAUDI ARABIA

In Partial Fulfillment of the
Requirements for the Degree of

MASTER OF SCIENCE

In

PIIYSICS

APRIL, 2016

KING FAHD UNIVERSITY OF PETROLEUM & MINERALS
DHAHRAN 31261, SAUDI ARABIA

DEANSHIP OF GRADUATE STUDIES

This thesis, written by **FATAI OLAWALE BAKARE** under the direction of his thesis adviser and approved by his thesis committee, has been presented to and accepted by the Dean of Graduate Studies, in partial fulfillment of the requirements for the degree of **MASTER OF SCIENCE IN PHYSICS**.

Thesis Committee

Dr. Khalil Harrabi (Adviser)

Dr. Shankar Kunwar (Member)

Dr. Watheq Ahmed Al-Basheer (Member)

Dr. Abdullah A. Al-Sunaidi
Department Chairman

Dr. Salam A. Zummo
Dean of Graduate Studies

28/4/16
Date

This work is dedicated to my late grand mother, Mrs. Sadatu Yusuf and my mom, Mrs. Bilikis Bakare.

ACKNOWLEDGMENTS

First of all, I am highly full of thanks , appreciation, and adoration to the government of the Kingdom of Saudi-Arabia, who through her extreme generosity had granted and financed my scholarship program at King Fahd University of Petroleum and Minerals. I pray Almighty Allah in His infinite mercy continue to bless, protect, and shower His mercy on this peaceful land, Saudi-Arabia.

Of course, my indebtedness knows no bound to my able Advisor, Dr. Khalil Harrabi, who scolded me often during my thesis work just to bring out the best in me; and never for once got tired of me. Always guiding, rectifying my mistakes and instructing me throughout my thesis work. Despite your hectic and tight work schedule, you still managed and carried me along. I am indeed grateful to you. thanks for being there sir.

My profound and undying thanks to my committee members, Dr. Shankar Kunwar and Dr. Watheq Ahmed Al-Basheer for their contributions, guidance, and patience during the completing of my thesis work.

My words of appreciation can not be completed without paying a big gratitude to the Director of Center of Research Excellence in Nanotechnology (CENT), Dr. Zain Hassan Yamani, for his invaluable trust, understanding and generosity towards me and my family during my course of study here in Saudi-Arabia.

I am also grateful to Prof. Ibraheem M. A. Nasser (Physics), Dr. Md. Abdul Aziz (CENT), Dr. Nasiruzzaman Shaikh M (CENT), Dr. Abbas Hakeem (CENT), Mr. Idris Akolade Bakare (CENT), Mr. Qasem Drmosh (CENT), Mr. Muhammad Ibrar Ahmed (CENT), Mr. Anas Karrar Jamil (CENT), Mr. Ganiyu Saheed Adewale (CENT), and Mr. Ganiyu Saheed Bukola (Clemson), for their endless support in my MS studies.

My heartiest gratitude to all friends in the department, the department of Physics at King Fahd University of Petroleum and Minerals.

Without me saying thanks to Nigerian Community, King Fahd University of Petroleum and Minerals chapter, then I must be an ingrate. If Nigerians continue to uphold brotherhood ties back at home as we do here, our nation will indeed be the best of all places to be. May Almighty Allah bless Nigeria, continue to bless the kingdom of Saudi-Arabia, and the world at large.

Strong Family ties is the bedrock of any society. To my entire family, Mom, Dad, all brothers and sisters, and all in-laws, thanks for always being there for me. To my Mom, Iyaniwura iye biye (the priceless mother), your are the most caring and supportive mother in the world. Even though, I haven't being at home for some years to see your health status, I know you do pray and ask over my well being on regular basis. Indeed, you are the most precious thing I have, and I pray to Almighty Allah to protect you for me and shower His mercy on you. You are more than a sweet-mother!

To my beloved wife, Faozeeyah Titilayo and my lovely and cheerful kids, Aisha Abimbola Bakare, AbdusSomod Adebayo Bakare, and Moryam Damola Bakare; of course, words alone are not enough to express my sincere and heartiest feeling to you all during my MS studies. May Almighty Allah mercy, protection, and blessings be on you all. My babies, you are always there for me!

TABLE OF CONTENTS

LIST OF TABLES

LIST OF FIGURES

THESIS ABSTRACT

NAME:	Fatai Olawale Bakare
TITLE OF STUDY:	Characterization of Dissipative States in niobium titanium nitride Superconducting Filaments
MAJOR FIELD:	Physics
DATE OF DEGREE:	April, 2016

Superconducting materials have potential application in radiation detection because of their special properties such as sensitive to incident radiation at optical wavelengths. Superconducting single-photon detectors (SSPDs) are those single-photon detectors that are sensitive to single-photon at visible and infrared wavelengths regime. These devices are highly promising for photon-registering technology for optical wavelength due to their high efficiency, high timing resolution, excellent recovery time as well as low dark count rate. These devices employ the concept of dissipative states in narrow superconducting materials. In this work, overcritical current pulses ($I > I_c$) have been used to create dissipative states, Phase-slip centers (PSC), in NbTiN superconducting filaments at different temperature below the critical temperature T_c. The voltage responses which initiated the the generation of the PSC were observed after certain delay time t_d. By employing a modified Time-Dependent Ginzburg-Landau (TDGL) theory, one is able

to analyze this time and subsequently deduced the time taken for the generated heat to escape the substrate τ_d. The τ_d was found to be independent of the temperature for all samples.

ملخص

المواد فائقة التوصيل لديها إمكانية تطبيقها في الكشف عن الإشعاع بسبب خصائص خاصة بها مثل حساسية للإشعاع الحادث في الأطوال الموجية الضوئية. كاشفات مصنوعة من فائق التوصيل للكشف على واحد حساسة إلى فوتون واحد في النظام المرئي وموجات الأشعة تحت الحمراء. هذه الأجهزة (SSPDs) الفوتون واعدة للغاية لتكنولوجيا تسجيل الفوتون لطول الموجة الضوئية نظرا لكفاءتها العالية وتفاصيل توقيت كبيرة وعروضه الممتازة الاحتفاظ الوقت وكذلك انخفاض معدل الظلام العدد الحالي الخاصة بهم. هذه الأجهزة تستخدم مفهوم مستويات المبددة في المواد فائقة التوصيل الضيقة. في هذا العمل، وكنا على الحرجة نبضات NbTiN ، في(PSC) جيم) لخلق مستويات المبددة، المراكز المرحلة الانزلاق Ic <I) التيار الكهربائي فائقة التوصيل يرثي في درجة حرارة مختلفة تحت ح درجة حرارة حرجة. وقد لوحظت ردود الجهد التي بعد معين الدفتيريا تأخير الوقت. من خلال توظيف نظرية تعديل وقت تابع غينسبورغ- PSC بدأت في جيل تمكنا من تحليل هذا الوقت وبعد ذلك استنتاج الوقت الذي يستغرقه لالحرارة المتولدة من (TDGL) لانداو الفرار من الركيزة. لقد وجدنا الوقت لتكون مستقلة عن درجات الحرارة العينات.

CHAPTER 1

INTRODUCTION

1.1 Superconductivity

Superconductivity is the phenomenon in which current flow without any loss of energy. It was first discovered by a Dutch physicist, Heike Kammerlingh Onnes, in 1911 [3]. Onnes observed that the electrical resistivity of a pure mercury wire drastically dropped to a very small measurable value at a certain temperature called the critical temperature T_c (see section 1.1.2) when he fed current through it and gradually reduced the temperature to about 4.2 K. This breakthrough has rapidly increased the technological application of superconducting materials; particularly, in medical applications of magnetic resonance imaging (MRI), in large scale magnetic guiding systems such as CERN, the presently constructed nuclear fusion energy plant ITER, in high throughput electrical power cables [4], as well as the maglev train presently in construction by Japanese Railways [5]. However, this unique characteristic of superconducting materials and many others, such as the observation of ideal diamagnetism, the appearance of quantized magnetic flux lines are destroyed when a large external source (more than the critical value), such as a current or magnetic field is applied to them [6].

It is well known that when a current is induced in a normal conductor, there would be energy dissipation in the conductor due to the collision of its electrons with the atoms in the lattice. This results to rapid decaying of the current. Unlike in conductors, in superconducting materials, an induced current will continue to flow due to the zero resistance. This current is discontinued when a current or magnetic field greater than the maximum value that the superconductors can withstand is applied. As a result, a transition from their superconductivity state to normal states is observed - this is termed as the destruction of superconductivity. This phenomenon is extremely useful in optical communication, particularly, in single photon detectors (SPDs) [2]. This technology benefits from the energy dissipation phenomena called phase-slip center (PSC) and hotspot (HS); which appear when a superconductor transits from superconducting state to normal state [2]. Further explanation is provided in section 2.2.

1.1.1 Dissipative Mechanism

The study of dissipative mechanisms in superconductors has attracted the interest of many investigators in attempt to understand the transition from superconducting state to the normal state. Among the dissipative mechanism in superconductors, flux flow (FF) is one of the most important phenomena which caused flux vortices, the surrounding of the normal core conductor or thin filaments by vortices of supercurrents [7]. When an unpinned superconductor carries a transport current in a uniform background fields, the transport current interacts with the flux quanta to apply a Lorenz force on each flux vortex. The moving flux vortices will induce an electric field and accelerate if there is no pinning force to balance the Lorentz force as a result the electric field increases with time. The transport current flowing through the normal cores of the moving flux vor-

tices is considered to be the cause of the dissipation [6]. In 1965, Bardeen and Stephen proposed a model which suggests that all dissipation occurs by normal resistivity in the central core of the flux vortices [8]. A more accurate analysis of the dissipative mechanisms was given by time-dependent Ginzburg-Landau (TDGL) theory which states that the process of flux penetration occurs through the suppression at the order parameter of the macroscopic scale [9]. It is shown that a superconductor carrying an electrical current larger than the critical current I_c (see section 1.1.3) for a considerable time can turn to the normal state [10]. The dissipative state is localized and can be considered as a PSC or a normal HS. Presently, the dissipative states in superconductors can either be created by laser light [11], magnetic field [12] or electrical current pulse technique [6].

1.1.2 Critical Temperature

When a material is cooled below a certain temperature such that its electrical resistance drops to zero, a phase transition from its normal state to a superconducting state is observed. The temperature at which the material loses it electrical resistance and changes phase is called the critical temperature (T_c). Superconductivity is destroyed (revert to normal state) above (T_c). The new phase (superconducting state) attained by the material is explained theoretically by John Bardeen, Leon Cooper, and Robert Schrieffer [13], commonly called the BCS theory. This theory will be discussed later in section 1.3. At low temperature, several materials, mostly metals and metallic alloys become superconductors at different T_c. Before the discovery of some high temperature superconductors by Georg Bednorz and Alex Muller [14], the highest critical temperature was close to 23 K. Currently, they are materials that can maintain their superconducting

state with critical temperature above the temperature of the liquid nitrogen (77 K).

1.1.3 Critical Current

Since zero resistance in a superconductor implies no energy loss, very thin materials such as superconducting filaments and superconducting thin films can be made to carry huge amount of current without breaking down. However, the superconductivity of the materials is destroyed when the applied current flowing through them exceed a certain maximum value called the critical current (I_c); (we are talking about below T_c obviously). The critical current current is a function of temperature; that is, more current flow when superconductors are cooled down.

1.1.4 Critical Magnetic Field

If a superconductor is placed in a weak magnetic field and cooled down below its T_c, the magnetic flux is completely expelled. If the field is very strong, the flux will penetrate the interior of the superconductor, thus destroying the superconductivity and the material will transit to its normal state. Similar to the I_c, a superconducting material will maintain it's superconducting property provided a critical magnetic field, H_c, is not exceeded. This critical value is the maximum magnetic field required to cause a dissipative state in a superconductor. The manner in which the superconductor is destroyed by the introduction of the field depends on the nature and the geometry of the the superconductor. The temperature dependence of the H_c is shown in 1.1. The curve H_c indicates the boundary between the superconducting and normal state.

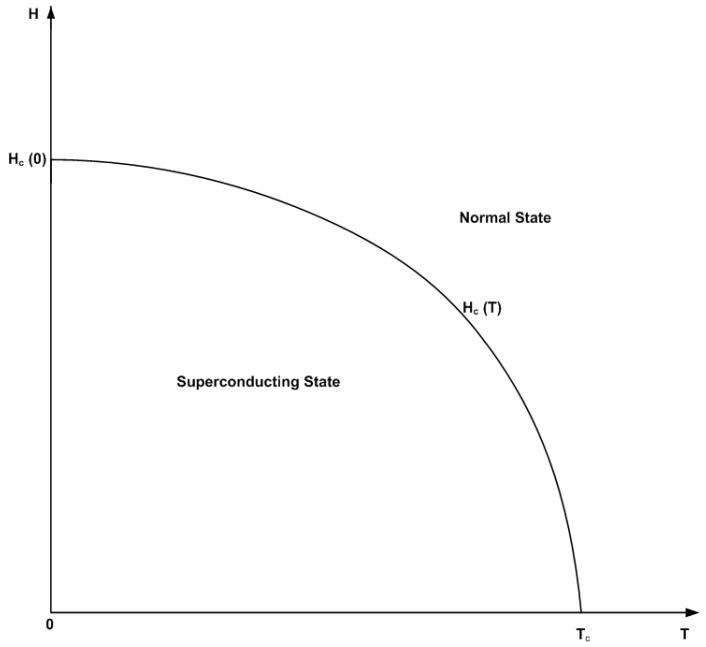

Figure 1.1: The temperature dependence of the critical magnetic field

1.2 Type I and Type II Superconductors

Basically, there are two types of superconductors which are distinguished by their T_c as well as their ability to exclude external magnetic fields from penetrating their interiors; these are commonly called Type I and Type II superconductors. The major difference between these two classes of superconductors is that the Type I has only one critical filed H_c whereas the Type II has two critical fields, H_{c1} and H_{c2}.

For Type I superconductors, their superconductivity state is maintained only below their T_c and below a ($\mathbf{H}_c$). Due to this, they are referred to as soft superconductors. Type I superconductor are mostly pure metals which are best described by the BCS theory [15].

On the other hand, the Type II superconductors behave differently when compared to their counterpart. They are made from alloys and can carry huge current as they possess higher $\mathbf{H}_c$. There is another class of superconductor which transit from the normal

state to the superconducting state at very higher temperature; this class of superconductor is called high temperature superconductor (HTS). It is also important to mention that the BCS theory cannot completely explain the superconducting property of this class of superconductor, as the Cooper pairs (see section 1.3) in these superconductors may be due to the antiferromagnetism of the cuprate materials.

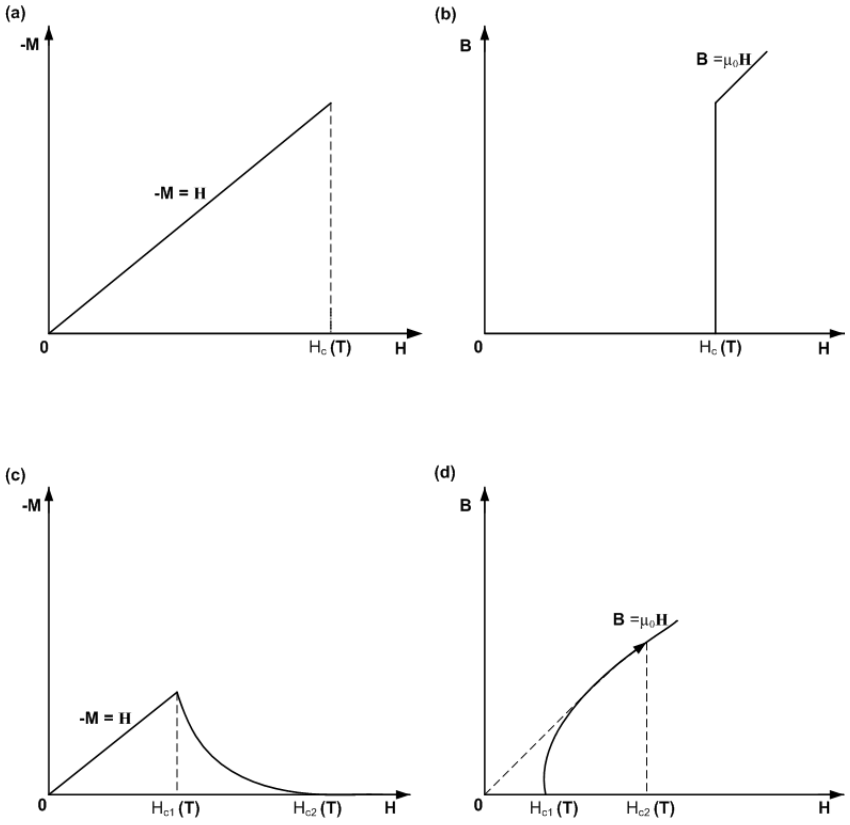

Figure 1.2: Schematic illustrations of magnetization (M) curves of (a and b) a type I superconductor and (c and d) a type II superconductor. For type I: Below H_c, (a) there is no flux penetration ($M = -H$), and (b) $B = 0$. Above H_c, (a) M drops to zero, and (b) there is perfect flux penetration. For type II: Below H_{c1}, the phenomenon is the same as in type I. However, between H_{c1} and H_{c2}, (c) M falls smoothly to zero, and (d) B smoothly rises to H. Above $H_{c2} > H_{c1}$, (a) M exponentially drops to zero, and (b) there is perfect flux penetration.

Unlike Type I superconductors, in Type II superconductors, when an applied magnetic field is increased from zero in them, two critical magnetic field are generated, $\mathbf{H}_{c1}$ and $\mathbf{H}_{c2}$ (as shown in Fig. 1.2 (c and d)). As depicted in Fig. 1.2(c), the applied field

penetrates the superconductors at the first critical field, $\mathbf{H}_{c1}$; however, their superconductivity is still maintained until above the second critical field, $\mathbf{H}_{c2}$. In between $\mathbf{H}_{c1}$ and $\mathbf{H}_{c2}$, there exist both normal and superconducting states in the material called a mixed state. This state is sometimes referred to as a vortex state.

It was mentioned earlier that to maintain superconductivity in a material, the vortices must be pinned. However, as the applied current or temperature is increased, movement of the vortices occurred. This motion is stopped by crystal boundaries as well as the microscopic defects (defects in the crystal lattice such as impurities, missing or misplaced atoms) in the materials, thus maintaining the superconductivity in the material [16]. The pinning of the vortices by the crystal boundaries and the microscopic defects is sometimes called flux pinning.

1.3 BCS Theory

In 1957, John Bardeen, Leon Cooper, and Robert Schrieffer [8] proposed a qualitative theory that explains the strange phenomenon of superconductivity; this is commonly called BCS theory. In their paper titled 'Theories of Superconductivity', they explained the reason why some materials lose electrical resistance at their critical temperature to become superconductors.

It is well established that in the normal state, electrons passing through the atoms of the lattice collide with the lattice and with one another. As a result, heat is generated and an increase in resistance is observed. However, in superconductivity state, the BCS theory states that these electrons paired up closed to the Fermi level to form what is known as Cooper pairs, and pass through the atoms of the lattice with zero electrical resistance. This theory also explained how the electrons are paired up. According to

this theory, when an electron passes through the crystal lattice of a superconductor, the positively charge ions in the lattice attract the electron thereby causing an inward distortion of the lattice. This electron attracts a closely passing electron that will also pass the distorted area prior to returning to its normal form. As a result, these electrons are paired up (Cooper pairs) and condensed by the atomic lattice vibration (phonons) into the same quantum state (i.e. all the electrons purpose the same energy). Unlike single electrons that are fermions which also obey Pauli's exclusion principle (no two electrons can exist in the same energy quantum state), the Cooper pairs have boson-like behavior and disobey Pauli's exclusion principle. From this, one can infer that the Cooper pairs are particles of integer spin. This can be simplified by the famous equation (Eq.1.1) in quantum mechanics, which describes the probability amplitude that both states "a" and "b" are occupied by electrons 1 and 2 in either order.

$$\Psi = \Psi_1(a)\Psi_2(b) \pm \Psi_1(b)\Psi_2(a) \tag{1.1}$$

Here the positive is required for boson-like (integer spin) particles and the negative for the fermions (half integer spin). One of the important information that can also be obtained from Eq.1.1 is that the Cooper pairs travel collectively and coherently as they are condensed to the same quantum state (i.e. when a = b in the above equation). It has long been confirmed that at low temperature the molecular movement of the ions in the crystal lattice is reduced. In line with this and provided that the superconductor characteristic temperature (T_c) is not exceeded, the Cooper pairs remain together. Otherwise, the Cooper pairs are broken and the superconductivity is destroyed.

1.4 Characteristic Lengths

There are two important characteristic lengths which one most mention when discussing concept of superconductivity. These are known as penetration depth and coherence length. The penetration depth is related to the electrons density of superconducting materials, λ. It is the distance required for the magnetic field inside a superconductor to reduce to 1/e the applied external field. While the coherence length, ξ, is related to the Fermi velocity of the superconductor as well as the energy gap (order of 10^{-3} eV) associated with condensation to the superconducting state. Above this length, the material loses its superconductivity. The ξ is useful to determine the transition thickness when a superconductor changes from its superconducting state to a normal state. The ratio of penetration depth to coherence length is the constant of the Ginzburg-Landau theory.

1.5 Objectives

In this study, an electrical current pulse technique was employed to achieve the following aims :

1. To study the creation of the dissipative states in niobium titanium nitride (NbTiN) superconducting filaments.

2. To measure the delay time in different samples (w = 3, 5 and 12 μm).

3. To deduce the heat escape time in the three samples (w = 3, 5 and 12 μm)

NbTiN is Type-II superconductor with a critical temperature about 8.3 K [17]. NbTiN superconducting filaments were chosen in this work owing to their short superconducting nanowire cooling time (τ_d), which is due to their relatively low resistivity above T_c compared to the first material used for SNSPDs, niobium nitride (NbN) [18]. Although niobium filaments (Nb) have shorter τ_d to NbN, but they suffer from latching (self-heating hotspot due to Joule heating) [19].

CHAPTER 2

PHASE-SLIPS CENTERS IN SUPERCONDUCTING FILAMENT

When the current in a superconducting filament is increased slightly above the critical current, an electric field appears. This field then accelerates the supercurrent above the critical current. As a result, the order parameter drops to zero, which allows the current to be carried as a normal current along the filament. As soon as the order parameter becomes zero, a voltage appears along the filament. This phenomenon was first observed by J.D. Meyer [20] on tin whisker as step-wise voltages on current-voltage (I-V) characteristics curves.

As it can be seen from some of their observation presented in Fig. 2.1(a), one note that each successive steps gives a consistence differential resistance $\frac{dU}{dI}$ value, which implies that there is a localized dissipative center along the filament and the phase difference of the order parameter slips on the two ends at different rate. The centers

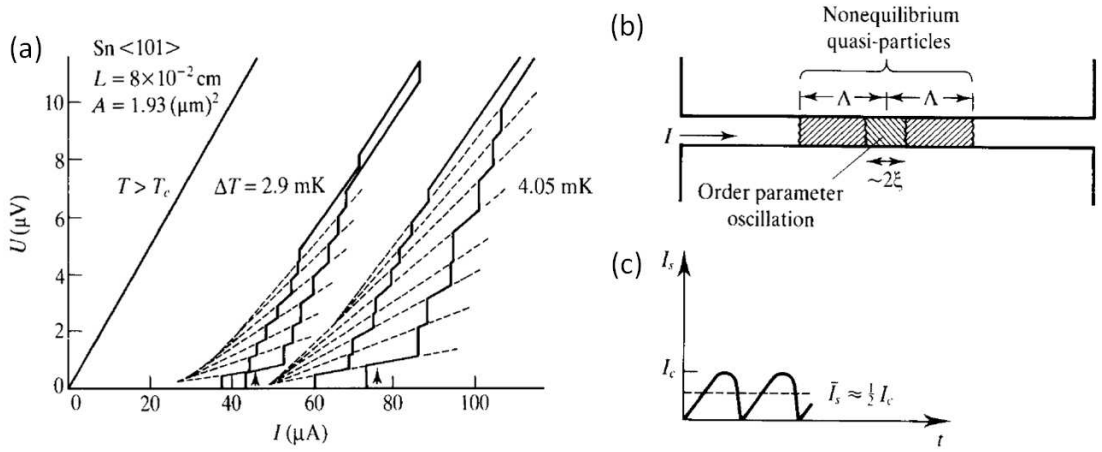

Figure 2.1: (a) Current-voltage (I-V) curve of tin whiskers showing step-wise structures due to the creation of Phase-slip centers. Here, $\Delta T = T_c - T$. (b) Schamatic illustration of a PSC-model prpoesed by SBT. The oscillation of the gap magnitude occured in a 2ξ-long core. Here the imbalanced charges produced as a result of nonequilibrium quasi-particles diffuse through a length of Λ. (c) Plot of superconducting current as a function of time in the core region with average value $\sim I_c/2$ [1].

at which this resistive state is nucleated are known as Phase-slips centers (PSC). The superconducting current I_s flows through the the filament without causing dissipation. This current is defined by $U = R_d(I - I_s)$ where $R_d = \dfrac{dU}{dI}$, the differential resistance, is independent of the current I. Similar observation was also reported by A. K. Elmurodov and his team. They studied experimentally and theoretically the transport properties of a superconducting NbN nanowire [21]. They found that by using different attached leads as superconducting contacts, the number of jumps in the I-V characteristics increases which indicates that the number of PSC modes increases.

In 1974, Skocpol et al [22] developed a model to explain the PSC concept. This model is known as the Skocpol-Basley-Tinkham (SBT)model. The Schematic illustration of the model is described in Fig. Fig. 2.1(b). Suppose the filament perfectly homogeneous, such that its critical current is equal everywhere. Since any slight increase in the bias current above the critical current will cause the order parameter to become zero such

that the entire current through the filament is a superposition of both the normal and superconducting current, the superconductivity will reappear and repeat a cycle; thus allowing a one-dimensional nanowires to be switched from superconducting to normal state. As a result, numerous non-equilibrium quasi-particles are created which subsequently diffuse over an inelastic length of the PSC. The generated quasi-particles cause overheating in the filament, thus creating a localized normal state or hot spot [22]. The model also pointed that at the center of the PSC, the phase difference of the order parameter slips by 2π [22].

To identify a PSC, the following features must be observed: (i) there is a delayed time t_d before the voltage along the superconductor appears in response to an electrical current pulse, which is the time required for the order parameter to collapse, that is the time needed to destroy the superconductivity; (ii) the voltage response suddenly jumps to a saturation value; (iii) the temperature at the center of the PSC is less than the critical temperature. The nucleation of PSC was confirmed in low-temperature superconductors [23]. Recently, phase-slip centers were observed [17] in the presence of an applied electrical current pulse. K. Harrabi [24] created a PSC after a certain delay time on a $YBa_2Cu_3O_7$ filament, by applying an overcritical current pulse $I > I_c(T)$. They employed the Tinkham modified TDGL model to obtain the heat escape time τ_{esp}. At low temperature, they found that the value of τ_{esp} to be 4 ns for 80 nm-thick film. This value was reported to be constant over the range 5 to 40 K. They attributed the loss of transmissivity at higher temperature to the of phonon-phonon decay.

In the case of an HS, one can identify it by the following features: (i) there is an increase in the voltage response with time after a certain delay time; (ii) usually preceded by nucleation of PSCs [23, 25, 26]; (iii) the temperature reached inside a HS is

larger than the critical temperature. Implying that in the HS region, a normal current flows.

2.1 Current dependence of temperature phase diagram for different dissipative modes

In this section, we discuss the behavior of the dissipative modes in which a temperature dependence of two threshold currents I_c and I_h is presented by a current-temperature phase diagram (Fig. 2.2). Here, the current I_c(T) and I_h(T) are plotted as functions of bath temperature T_b. The critical current I_c is the current giving the longest observable delay, it is the threshold for the nucleation of PSC [1]. While, the current I_h is defined as the minimum threshold current whose Joule effect is sufficient to maintain a localized normal zone above T_c [27, 25, 26].

At region close to T_c, when T/T_c approaches unity, I_c varying from $(1 - T/T_c)$ to $(1 - T/T_c)^{3/2}$[27, 25]. However, at temperature very close to T_c, the dependence temperature of I_h is defined as function of $(1-T/T_c)$. At lower temperatures, I_c increases more suddenly than I_h thus $I_c > I_h$ (as shown Fig. 2.2). Whereas, on increasing the bath temperature close to T_c (see point B in Fig. 2.2 a & b) the current I_c rapidly drops below I_h, in this case $I_c < I_h$ (see blue shades in Fig. 2.2 a & b)). In this region, one observe that PSC naturally evolves into a localized normal zone or hot spot as the current increases significantly over I_c, thus resulting in an internal temperature larger than T_c [23, 25]. At $T < T^*$ (point A in Fig. 2.2 a) and when $I_h < I < I_c$, a voltage signal appears after a certain delay time which results in the nucleation of a fast PSC (see the left orange shade in in Fig. 2.2 a) that immediately transforms into an HS.

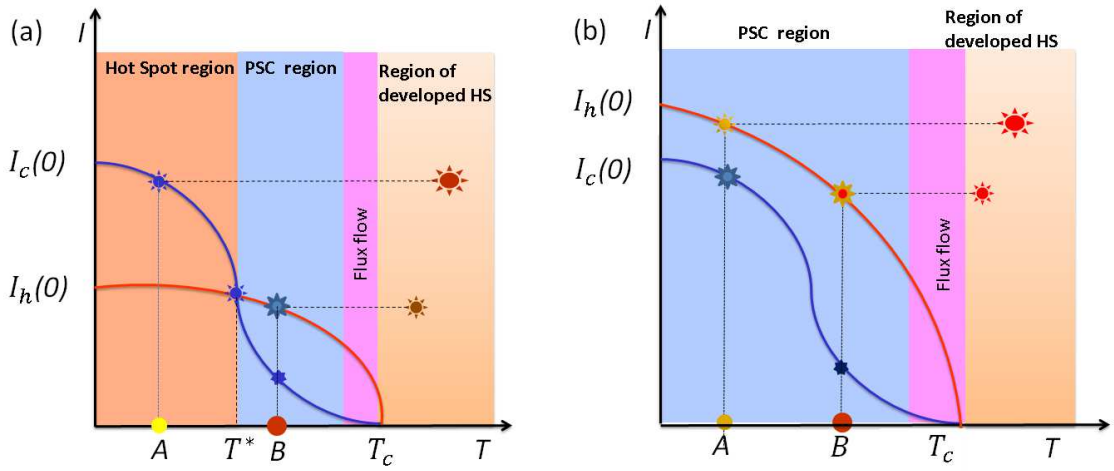

Figure 2.2: Current dependence of temperature phase diagram illustrating the different dissipative regimes of flux flow, PSC and HS. (a) when a HS is created first. (b) when no HS was observed at the onset when the current amplitude was increased above the critical current I_c. Here, I_c is the critical current which is the current that initiates the dissipation. I_h is the threshold current required to maintain a steady HS above the critical temperature T_c. While T^* is the tempereauter at which a steady HS is initiated which is when $I_h(T^*) = I_c(T^*)$.

At $T > T^*$ (point B in Fig. 2.2 a) and when the current is slightly increased such that $I_c < I < I_h$, gives rise to a PSC whose length is determined by the quasi-particle inelastic diffusion range given by $L_n = 2\Lambda = v_F(\tau_c\tau_r/2)^{1/2}$, where v_F is the Fermi velocity, τ_c is the elastic collision time, and τ_r is the transverse inelastic relaxation time. This length was interpreted by Skcopol et al [22] as the length of non-equilibrium through which normal currents flows. As soon as the PSC is created and the I_h is reached, the PSC abruptly transforms into an HS. This was later verified experimentally in 1995 by Peterson *et al.* [28]. They studied the I-V characteristics associated with self-heating HSs in HTS thin films under both current-biased and voltage-biased conditions.

Experimentally, the measurement of I_c at $T_b < T_c$ is obtained by increasing the input current from a signal generator until a resistive regime appears indicated by the

voltage rise in the filament (see chapter 4).

2.2 Application of Phase-Slip centers

Some of the amazing technological benefits of the phase-slip centers are their application in thermal radiation, astronomy, as well as optical communication [29].

For example, the basic principle of dissipative state such as PSC is widely used in bolometer, an electrical resistance thermometric device used to measure the temperature of a radiation absorber. The bolometer employs the temperature dependence of the resisitivity of materials to measure the temperauter of the radiation absorber. In this device, superconducting filaments are used as radiation absorber and thermometer. For instance, Clarke et al [30] used an Al and and a Bi film deposited on a sapphire substrate supported by nylon as a thermometer and radiation absorber, respectively, to optimized a superconducting bolometer for near millimeter waves.

In optical communication,superconducting single photon detectors (SSPD) have been widely used in various field such as optical quantum information (QI) application. For example, in optical quantum information technologies, individual quantum particles such as photons are used to encode and manipulate information. A SSPD is a device used to detect a single photon at visible and infrared wavelength regimen with a fast recovery time. The mechanism of SSPD is based on the generation of an electrical signal upon the absorption of a photon (as shown in Fig. 2.3). The energy of the absorbed photons causes a non equilibrium state which is followed by hot excited quasi particles at temperature larger than that of the Cooper pairs in the superconductor. An equilibrium state is attained by following relaxation process: (i) electron-electron interaction and electron-phonon interaction cause inelastic scattering of quasi-particles,

(ii) quasi-particles are generated by phonons, (iii) recombination of quasi-particles and (iv) generated heat escapes to the substrate by the phonon in the superconductor.

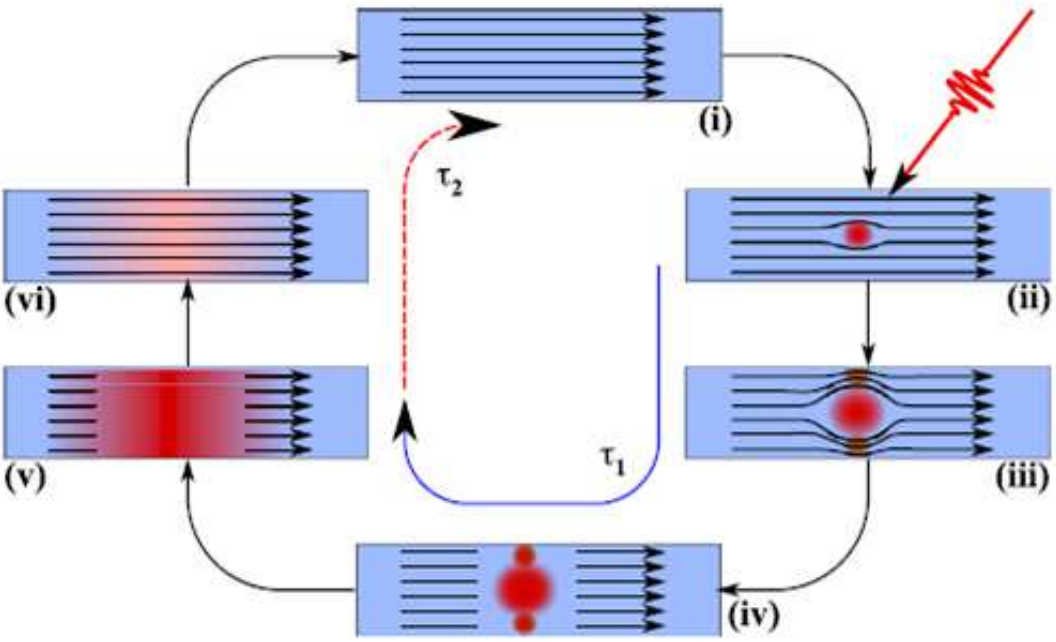

Figure 2.3: Schematic illustration of the mechanism of the superconducting nanowire single-photon detector (SNSPD). (i) The superconducting nanowire is maintained well below the critical temperature and the direct current (DC) biased below the critical current. (ii) When a photon is absorbed by the nanowire a resistive hotspot is created. (iii) The created hotspot forces the supercurrent to flow along the resistive region. Since the superconducting strips used for this device are narrow, the local current density around the hotspot increases, exceeding the critical current density. (iv) As a result, a resistive barrier across the width of the nanowire is formed. (v) Along the axis of the nanowire, Joule heating (via the DC bias) aids the growth of the resistive region until the current flow is blocked and the bias current is shunted by the external circuit. (vi) This allows the resistive region to vanish and the wire becomes fully superconducting again. Finally, the bias current flowing through the nanowire returns to its initial value (i)[2].

CHAPTER 3

EXPERIMENTAL SETUP

3.1 Sample fabrication and characterization

3.1.1 Fabrication

The NbTiN thin film purchased from STAR-Cryoelectronics Company (NM, USA), was grown on sapphire at room temperature by DC magnetron sputtering of NbTi target under the atmosphere of argon-nitrogen plasma. Thereafter, two lateral probes of 1 mm partially apart, and four contacts pads made out of gold were patterned in the top of the NbTiN film using standard photo-lithography and ion milling techniques. The samples used in this work have different widths: 3, 5, and 10 μm; labeled as BK-NT3, BK-NT5, and BK-NT10 corresponding to their respective width. Fig. 3.1 shows the schematic illustration of the NbTiN sample that was used for this study.

3.1.2 Characterization

The sample connection to the cables terminal was made using a thin copper wire with indium soldering. The resistance temperature (R-T) measurement and voltage pulse response were carried out in a 4 K closed-cycle cryostat under vacuum with a temperature

controller. The operating temperatures T_b for these measurements were varied from 4.1 K to critical temperatures, T_c. In order to ensure a good thermal contact between the sample and coldilate, we greased the sample stage with some vacuum grease prior to the sample mounting.

The R-T measurements were conducted to determine the resistivity and the T_c of the samples using a four-point probe technique (as shown in Fig.3.1a).

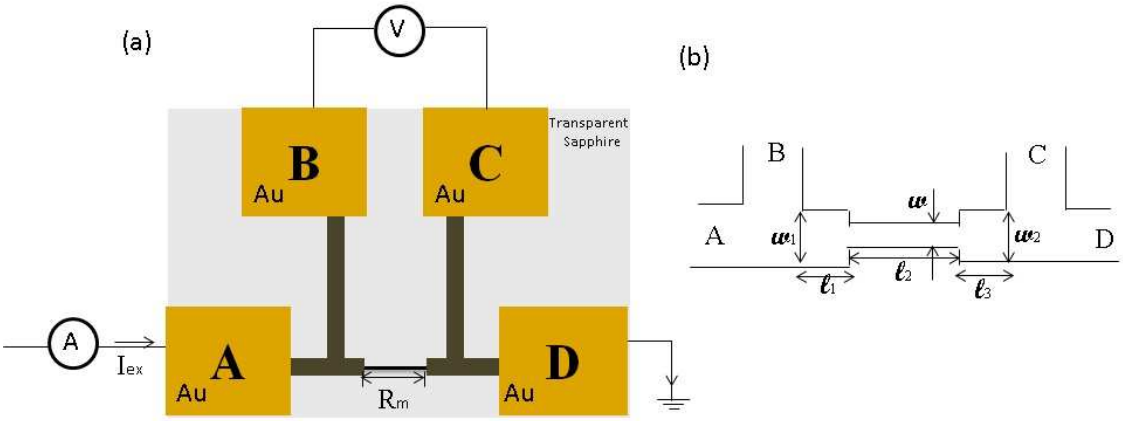

Figure 3.1: Schematic illustrations of (a) R-T measurement using four-point probe technique. (b) resistivity calculation along the narrow bridge of the three samples with $w = 3$, 5, and 10 μm. Where $w_1 = w_2 = 20$ μ m and $l_1 = l_3 = 100$ μ m

A 1 μA DC current, I_{ex}, was sent from a Current source KEITH-225 to the NbTiN filament from the input probe A to the ground via the output probe D. The voltage across the filament, V_i , was measured between the two lateral probes (see Fig.3.1a) using an Agilent-34401 digital multimeter. The measured resistance between these two lateral probes was calculated using $R_m = \frac{V_i}{I_{ex}}$. Fig. 3.1b shows that the R_m is a combination of some section of the filament l_1, l_3 and the bridge, l_2, which is equal to $R_m = R_1 + R_2 + R_3$. Furthermore, the resistivity of the samples were calculated from the following equation:

$$\rho = \frac{R_m b w_1}{2l_1 + l\frac{w_1}{w}} \tag{3.1}$$

where b, w_1, l, and l_1 represent the thickness, width of the NbTiN film having length, $l_1 = l_3$ =100 μm is the length of NbTiN having width $w_1 = w_3$.

Fig. 5.1 shows the curve of resistivity as a function of temperature (see appendix) when a DC current of 1 μA is sent to the three NbTiN samples : BK-NT3, BK-NT5, and BK-NT10.

From the R-T measurements, the T_c and the residual resistivity (at normal state) ρ for the three samples are presented in Table 3.1

Sample	Width w (μm)	T_c (K)	ρ (15 K) ($\mu\Omega.cm$)
BK-NT3	3.00	8.30	182.0
BK-NT5	5.00	8.60	158.0
BK-NT10	10.00	8.50	77.0

Table 3.1: Corresponding width w, T_c, and ρ (at 15 K) for the three NbTiN samples: BK-NT3, BK-NT5, and BK-NT10.

3.2 Experimental Set-up

Fig.3.2 shows the schematic illustration of the experimental set-up that was used for this study. The experimental set-up is made up of a fast pulse generator (AVETEC E3A-B) used for sending an electrical pulse of 450 ns duration at a repetition rate of 10 kHz through 50 Ω coaxial cables, a delay lines of 240 ns was employed to separate the incident pulse (V_i) from the reflected one (V_r) at the sample stage, an external attenuator, varying by 0.1 dB steps, was incorporated in the circuit to change the voltage pulse, the voltage response as well as the delay time t_d were measured using a 1

GHz oscilloscope (Agilent InviniiVision 6000 Series), and a temperature controller was used to change the temperature of the sample holder.

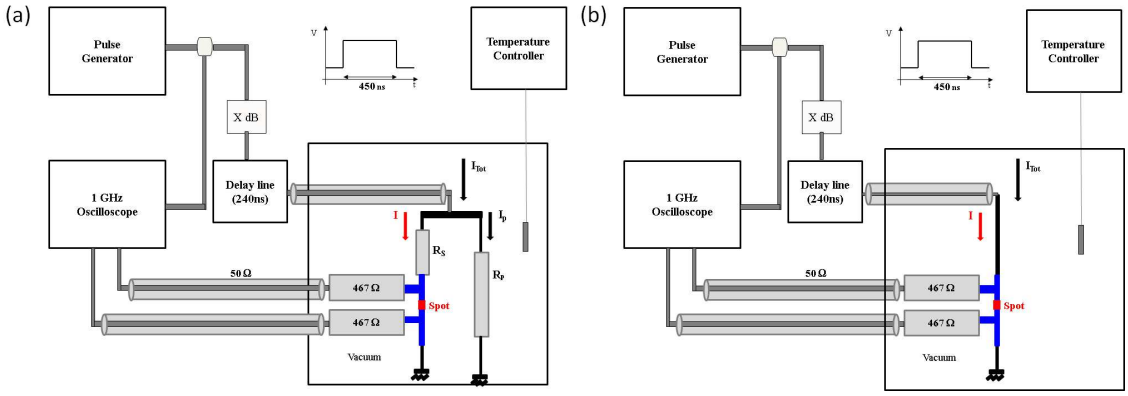

Figure 3.2: Schematic illustration of the experimental set-up used for pulse measurements (a) with the combination of both R_s and R_p. (b) without the combination of both R_s and R_p

When an incident pulse is sent from the a pulse generator, a pulse, known as reflected pulse V_i, is reflected from the ground. The nature of this pulse depends on the load at the cable end, which can be understood using, $\frac{V_r}{V_i} = \frac{R-Z_0}{R+Z_0}$, where Z_0 is the coaxial cable impedance ($Z_0 = 50\ \Omega$). From this relation, the following conclusion can be deduced:

(i) when there is no load ($R = 0$) at the coaxial cable end (see Fig. 3.2b), V_r appears in the oppose direction and with the same magnitude as V_i, that is, $V_r = -V_i$.

(ii) if the coaxial cable end is open at one end ($R = \infty$), we observed that $V_r = V_i$.

(iii) the last configuration is when there is a load at the other end of the cable ($R = Z_0$), for this case, $V_r = 0$ (as shown in Fig. 3.2a) which means that there would be no reflected pulse appearing.

In order to cancel out the reflected pulse, a combination of large series resistor R_s and a parallel resistor R_p ($R_s = 187\ \Omega$ and $R_p = 67\ \Omega$) were used (as shown in Fig. 3.2), which is equivalent to a 50 Ω impedance at the line's termination. This was also used

to maintain a constant bias current flowing into the sample. Two 467 Ω were connected in series through lateral electrodes to the oscilloscope to prevent current leakage into the oscilloscope and allowing steady flow of the current through the sample bridge to the ground.

By assuming that there is no current loss in the coaxial cables and the ohmic contacts are negligible, the current flowing through the sample in the superconducting state is given by $I = I_{Tot}R_p/(R_p + R_s)$, where $I_{Tot} = \frac{V_i}{Z}$ (the line impedance Z=50 Ω, (V_i) is the input voltage).

CHAPTER 4

RESULTS AND DATA ANALYSIS

4.1 Characterization of dissipative states in NbTiN superconducting filament

We measured the voltage responses of sample BK-NT3 at T_b and for currents larger than the critical current I_c. The current was sent from probe A to the ground (probe D), as shown in Fig. (3.1). The difference of potential was measured between the probe B and the ground. The critical current is determined from the experiment as the minimum current that requires the voltage response to appear and it is about 1.80 mA. We also interpreted it as the current that produces the longest attainable delay time which is the 450 ns used in this setup.

When the input current value increased slightly above I_c (I_c = 1.80 mA), one observed the appearance of the first voltage response which begins with an inductive peak due to the inductive wire we used to connect the coaxial cable to the sample. It

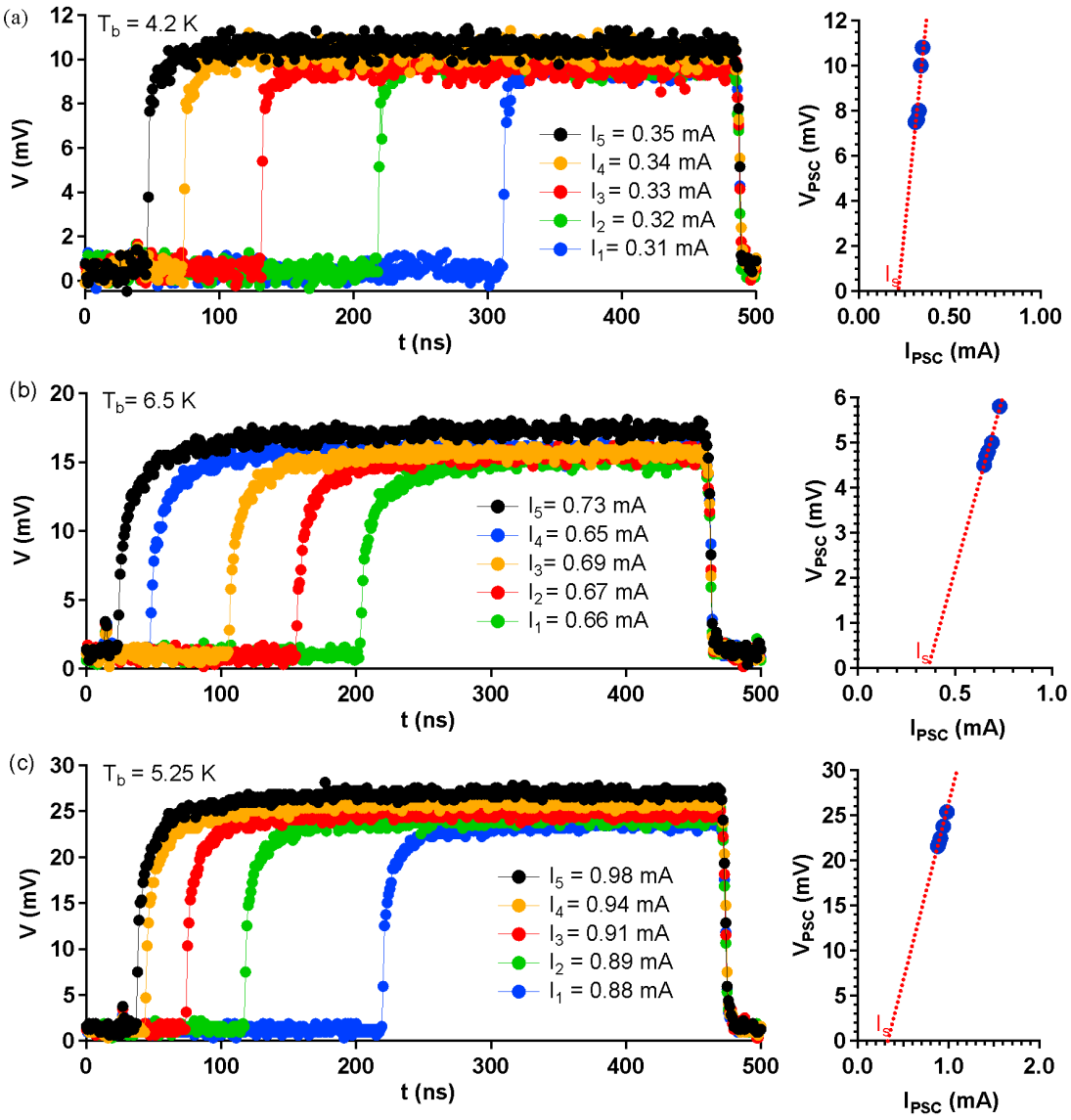

Figure 4.1: (a) Voltage response plotted as a function of time at different temperature and different current value above I_c for the three NbTiN samples:(a) BK-NT3 ($w = 3\mu$m), (b) BK-NT5 ($w = 5\mu$m), and (a) BK-NT10 ($w = 10\mu$m). t_d is the time which precedes the appearance of the voltage response. The plot of V_{PSC} against I_{PSC} for each of the samples is presented on the right, where $I_s \simeq 0.4$ mA

is followed by a state $V = 0$, then an abrupt voltage increases and reaches a saturation point and remains constant. We interpret this mode as PSC based on the stated features [17]. By increasing the current amplitude, the t_d decreases until it reaches a small value (see Fig. 4.1a).

From Fig.4.1b, we obtain two important parameters to determine the heat dissipated in the localized zone. The first one is the differential resistance $\frac{dV}{dI}$ which shows consistency of the pulse generated. This resistance was found to be $\sim 12.1\ \Omega$ for sample BK-NT3. By extrapolating the linear plot of V_{PSC} versus I_{PSC}, one gets another interesting parameter, the superconducting excess current $I_s \sim 23\ \mu$A. Since the PSC is interpreted as an oscillation of the order parameter at the Josephson frequency between 0 and 1, we can infer that the total current is the superposition of two currents, the superconducting and the normal current. From these parameters, we can estimate the heat dissipated at the localized zone per unit volume using $\rho I(I - I_s)/(w.b)^2$. Similar steps were taken for samples BK-NT5 and BK-NT10 (see the figures on the right of Fig 4.1b and 4.1c). The corresponding I_s for these samples are $\sim 37\ \mu$A and $\sim 37\ \mu$A, respectively.

Fig. 4.2 depicts the curve of the measured I_c for the three samples as a function of temperature. However, the value of I_h at $T_b > T_c$ can be obtained from the experiment by increasing the current beyond I_c until the flat voltage of PSC changes to a rising voltage indicating a HS [23].

On the other hand, the experimental measurement of I_h at $T_b < T^*$ is not straightforward. It requires two pulses generator for sending both short and long pulses with time. From the pulse generator for sending short pulse, short pulse of intensity larger than I_c is sent through the filament which results in the nucleation of a rising voltage of HS on the same spot of the filament. Thereafter, a long pulse with small intensity is sent. The followings are observed depending on the configuration of the return current I_r following the experimental measurement of I_h at $T_b < T^*$: If the $I_r > I_h$, an increasing voltage appears which is interpreted as an expanding HS. On the other hand, if the

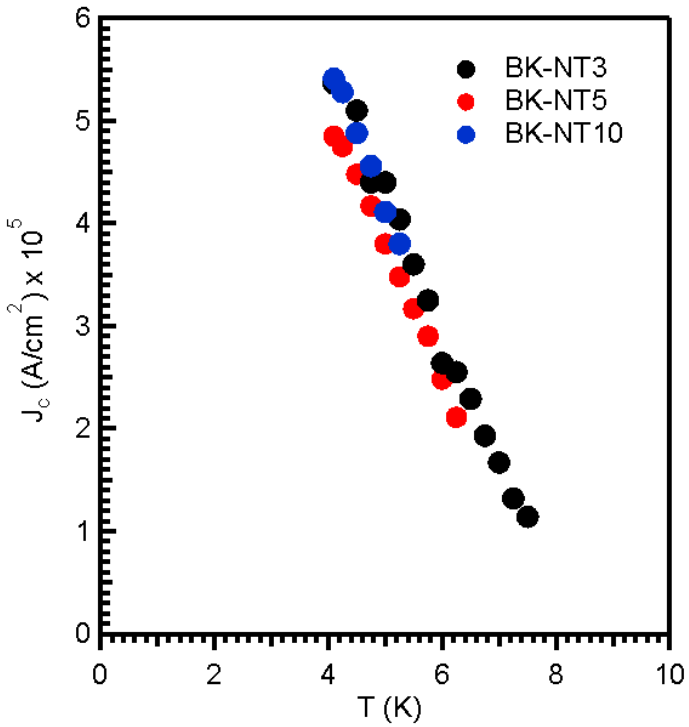

Figure 4.2: Measured critical currents density plotted as a function of temperature for the three NbTiN samples

$I_r < I_h$, a descending of HS is observed. This implies that the current that gives the steady level of HS determines I_h and this is obtained from the voltage on the long pulse.

For instance, Harrabi, *et al*. [31] created a phase slip center and hotspot on a 80 nm-thick $YBa_2Cu_3O_7$ nanowire deposited on two different substrate, sappire and MgO, by applying a current larger than the critical current through the nanowire. Their findings provide the information for obtaining the maximum bias current, return current as well as the rate required for an HS to decay. By analyzing their experimental results with TDGL theory, they found the time required for the PSC to be nucleated to be 6ns and 75 ps/ nm for YBCO on sapphire and MgO, respectively.

4.2 Measurement of heat escape time

As established in the previous section, we noted that increasing the input current causes the t_d to shrink until it becomes extremely small. In this section,the trend that this observation follows for the three different samples: BK-NT3, BK-NT5, and BK-NT10 will be described by following the work of Pals and Wolter [32] and subsequently obtain the relaxation time τ_d. By solving the one dimensional Time-Dependent Ginzburg-Landau (TDGL) equation [33] and neglecting its space dependence, one obtain a simplified equation for the order parameter:

$$\frac{df}{dt} = \frac{1}{2\tau_d}\left(1 - f^2 - \frac{4}{27f^4}\left(j_s/j_c\right)^2\right) \tag{4.1}$$

In Eq. (4.1), f is the order-parameter normalized to its equilibrium value f_{eq}, τ_d is the relaxation time, j_s is the superconducting current density, and j_c is the critical current density. From the above equation, we make the following remarks. When $j_s < j_c$, the f tends to its limiting value, $f \sim 1$. As a result, one observe no voltage appearance. However, when $j_s > j_c$, f begins to fall from 1 to 0. In this situation, a voltage begins to appear along the filament. The appearance of this voltage takes some time after the onset of the input current. We interpreted this time as the t_d in this experiment. Eq. (4.1) can be simplified into an integra form:

$$t_d(I/I_c) = \tau_d \int_0^1 \frac{2f^4 df}{\frac{4}{27}(\frac{I}{I_c})^2 - f^4 + f^6} \tag{4.2}$$

where the prefactor τ_d was interpreted as the inelastic electron-phonon relaxation time τ_E in the normal state close to the critical temperature and the time, the integration limits describe the behaviour of variable f which varies from 1 to 0. One limitation

in Eq. (4.2) is that it can not fit values of $t_d \leq \tau_d$. This implies that a modification is required on Eq. (4.2). In order correct the invalidity of this equation for $t_d \leq \tau_d$, Tinkham [33] developed a modified theory where temperature dependent of τ_d was put into consideration and the numerator of the integrand in Eq.(4.2) was replaced by

$$2f^4 + 1.65f^5 - 0.5(I/I_c)^2 \tag{4.3}$$

As a result, the t_d became dependent on the two variables $\mathrm{T/T}_c$ and $\mathrm{I/I}_c$. This modified TDGL theory by Tinkham was employed throughout this work for fitting the experimental data of t_d. The experimental values t_d were plotted as a function of $\mathrm{I/I}_c$ and fitted with the simplified Eq. (4.2). The prefactor τ_d was deduced subsequently.

After the nucleation of the dissipative state, the heat generated then flow through the filament by thermal conduction and evacuated to the substrate by means of phonon radiation. To effectively deduce the τ_{esc}, both phenomena need to be considered for its deduction. For the heat transferred through the filament, its power dissipation P_f is given as:

$$P_f = \frac{\int C_e dT + \int C_p dT}{\tau_d} \tag{4.4}$$

here C_e and C_p are the respective specific heat of electron and phonon. The τ_d retain is usual meaning as in Eq. (4.1). The power dissipation when the heat is being evacuated to the substrate P_s can be written as:

$$P_s = \frac{\int C_p dT}{\tau_{esc}} \tag{4.5}$$

By assuming that $P_f = P_s$ during the dissipation, one can obtain the τ_{esc} by equating

both Eq. (4.4 and 4.5):

$$\tau_{esc} = \tau_d \left(\frac{C_p}{C_e + C_p} \right) \tag{4.6}$$

4.3 Temperature dependence of the phonon escape time

We studied the behaviour of the τ_{esc} as a function of temperature for the three samples. For all the samples, we observed that the τ_d is almost independent of T_b, each of the data are presented in both Fig. 4.3 (see Appendix for the plots of other temperatures).

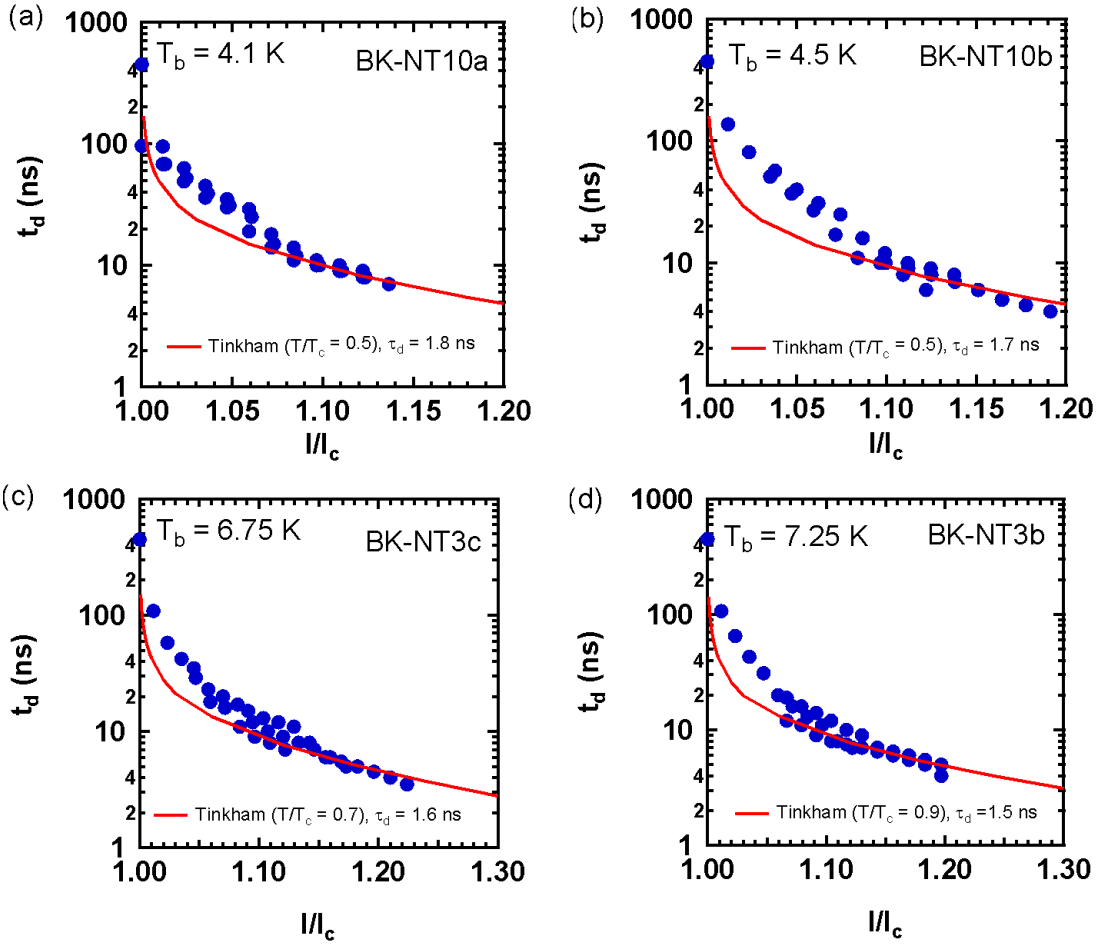

Figure 4.3: Delay time t_d as a function of I/I_c at different T_b in sample BK-NT10 (a & b) and BK-NT10 (c & d). The t_d axis is in logarithm scale. The solid curve is the Tinkham's fitting obtain from Eq. (4.2) Here the τ_d is the prefactor of Eq.(4.2)

The τ_d values for the widest sample (BK-NT10) at the different T_b as shown in Fig. 4.1 (a - d) were found to be around 1.75 ns. The above procedure was followed for samples BK-NT5 (see Appendix). The overall behaviour of the deduced τ_{esc} for the whole temperature range will be shown in section 4.3. The graph of τ_d versus T_b as depicted in Fig. (4.4) gives a constant trend which explains that τ_d is independent of T_b. The different values of τ_d for the three samples are presented in Table 4.1. However, due to weak signal at $T_b \sim T_c$,we were prevented from performing such measurements.

Sample	Width w (μm)	T_c (K)	τ_d (ns)
BK-NT3	3.00	8.30	1.3
BK-NT5	5.00	8.60	1.1
BK-NT10	10.00	8.50	1.7

Table 4.1: τ_d values for the three NbTiN samples with their corresponding specifications.

The phonon escape time τ_{es} can be deduced from τ_d by considering the transfer of heat from the film to the substrate which is dominated by the phonon escape and along the film which is dominated by electrons and phonons. If the total of specific heat of C_ϕ and electrons C_{el} equals to $C = C_\phi + C_{el}$, then the phonon escape time is given by a relation $C_\phi/\tau_{es} = C/\tau_d$ [25].

The behavior of gap relaxation time (thus the phonon escape time) to a temperature change below the critical value is depicted in Fig. 4.4a for sample BK-NT3. It is seen that the τ_d is constant (dotted line) as the temperature is increased in the range of 4 K to 7.25 K. This defines that prefactor τ_d is a T-independent parameter. The same behavior was also observed in Fig. 4.4b and Fig. 4.4c for samples BK-NT5 and BK-NT10, respectively, although the values of τ_d are a slightly different.

The phonon escape from the film to the substrate is considerably influenced by phonon-phonon scattering in addition to the acoustic mismatch between two lattices

and the defects of the interface. If the average phonon energy reaches a rounding domain in the dispersion relation due to a temperature rise, many channels will open for phonon decay compared to that of the linear relation. Yet, at the same time the phonon evacuation could also be decelerated because a temperature rise will create numerous phonons so that they impede one another causing phonon transport to become diffusive rather than ballistic. Nevertheless, since the range of temperature of NbTiN is still in the Debye regime, the phonon dispersion relation is linear and phonon-phonon scattering is only a few. Thus, the elevation of temperature does not influence the phonon escape.

4.4 Dissipation Inside PSC

In order to estimate the temperature of the PSC centre T_m, we took into account both the reduced dissipation rate $\rho I(I - I_s)$ and the heat transfer along the filament $\int C_{es}(T)dT$, where C_{es} is the specific heat of excess electron. Here the integral boundaries ranges goes from T_b to T_m. Since there is electric field penetrating into the superconducting filament, one needs to incorporate the inelastic diffusion length Λ into the aforementioned relations. The result of this combination allows the determination of the temperature inside the PSC centre:

$$\frac{VI}{w \times b \times 2\Lambda} = \frac{\rho I(I - I_s)}{w^2 b^2} = \frac{\beta(T_m^4 - T_b^4)}{4\tau_{esc}} \tag{4.7}$$

where V is the PSC voltage, β is constant in the Debye regime.

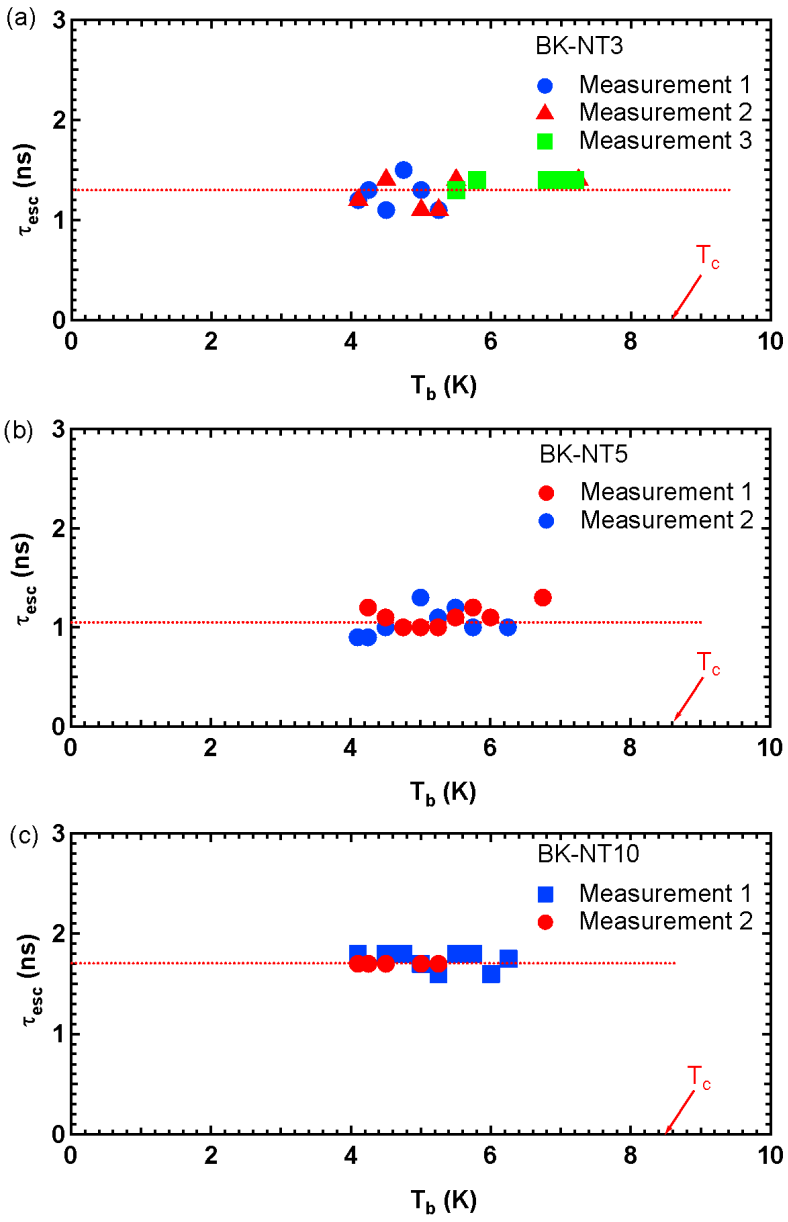

Figure 4.4: Heat escape time τ_d as a function temperature: (a) BK-NT3. (b) BK-NT5. (c) BK-NT10

CHAPTER 5

CONCLUSION

We have measured the heat escape time of 20 nm-thick niobium titanium nitride filaments deposited on sapphire with different width at different temperatures, by employing a current pulse technique to create dissipative states. A pulse current was sent to the sample using a signal generator via a 50 Ω coaxial cable. In order to maintain a contain biased current flowing through the filament, in one of our experimental setup, we connected a large resistor in series with the sample and a shunt. We characterized our samples by measuring the I-V characteristic behavior. The critical temperature of each of the three samples were obtained from the resistance - temperature measurements were found to be in closed range of 8.3 K to 8.6 K. We investigated below the critical temperature of each the superconducting filaments and found that by applying a current below the critical current generates no voltage response, which indicates that the filament is still in the superconducting state. However, slightly above each of these temperatures, a voltage appears which indicates the destruction of the superconductivity. This dissipative voltage appeared in a localized spot, phase slip center, after a certain delay time t_d. The PSCs are characterized by an increase of the voltage as a

function of time.

The time of creation of the PSCs were analyzed using the Time-Dependent Ginzburg-Landau equation and was found to be independent of the temperature in the Debye regime of our filaments. From this model, we estimated the heat escape time for the three 20 nm-thick NbTiN samples. In this work, we were unable to observed the nucleation of an hotspot. This was attributed to insufficient threshold current needed to initiate an HS after the nucleation of a PSC.

Appendix A

RESISTANCE-TEMPERATURE MEASUREMENT

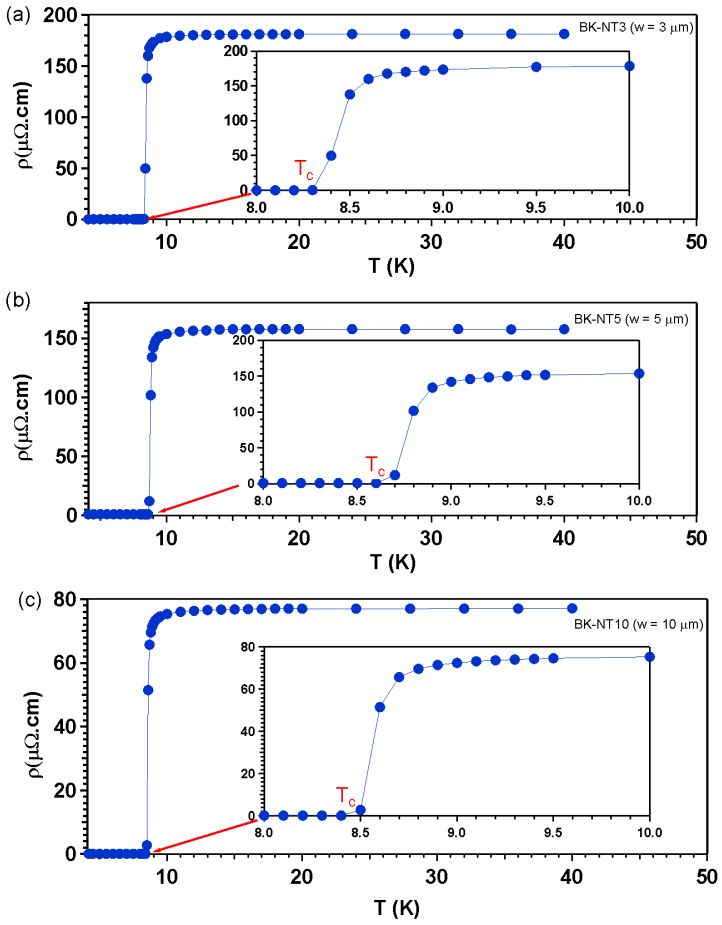

Figure 5.1: Resistivity as a function of temperature for three different samples: (a) BK-NT3, (b) BK-NT5, and BK-NT10, respectively. The insets depict the resistivity of each sample close to T_c.

Appendix B

VOLTAGE RESPONSE FOR DIFFERENT TEMPERATURES

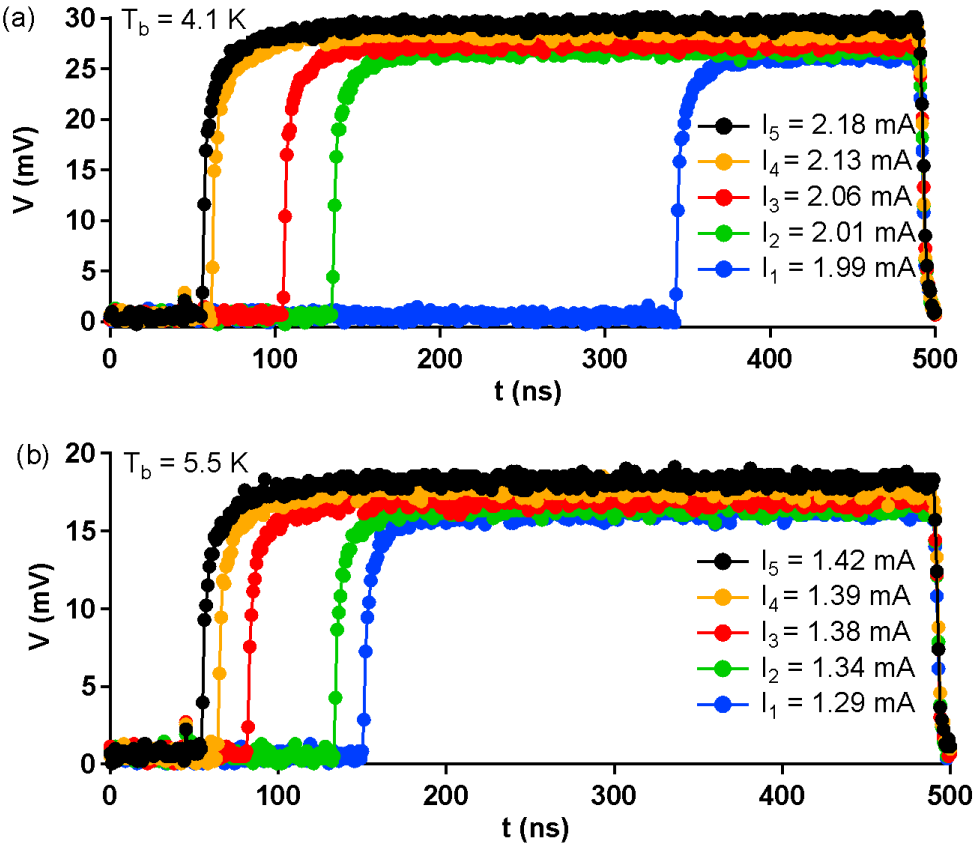

Figure 5.2: Voltage response plotted as a function of time at different temperature and different current value above I_c for the NbTiN samples of 3 μm-wide, BK-NT3

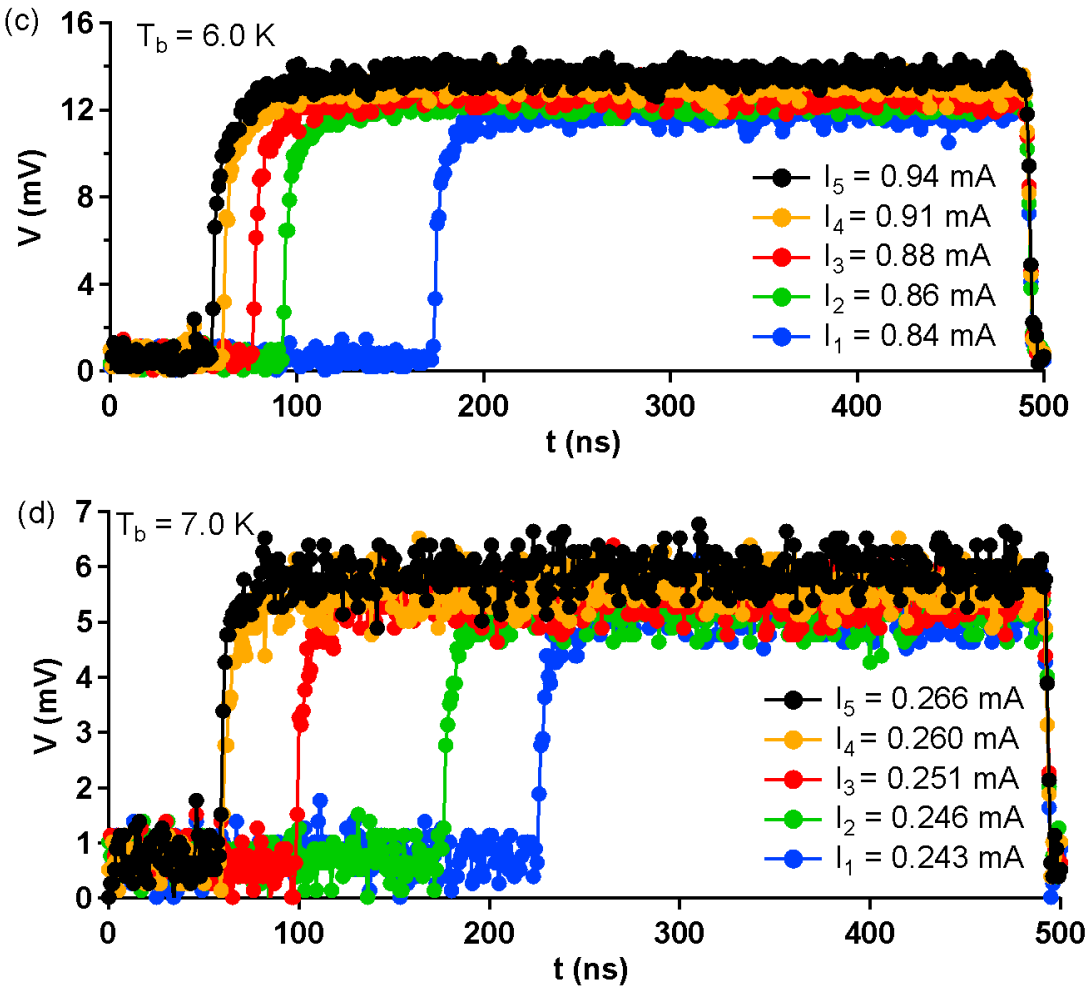

Figure 5.3: Voltage response plotted as a function of time at different temperature and different current value above I_c for the NbTiN samples of 3 μm-wide, BK-NT3

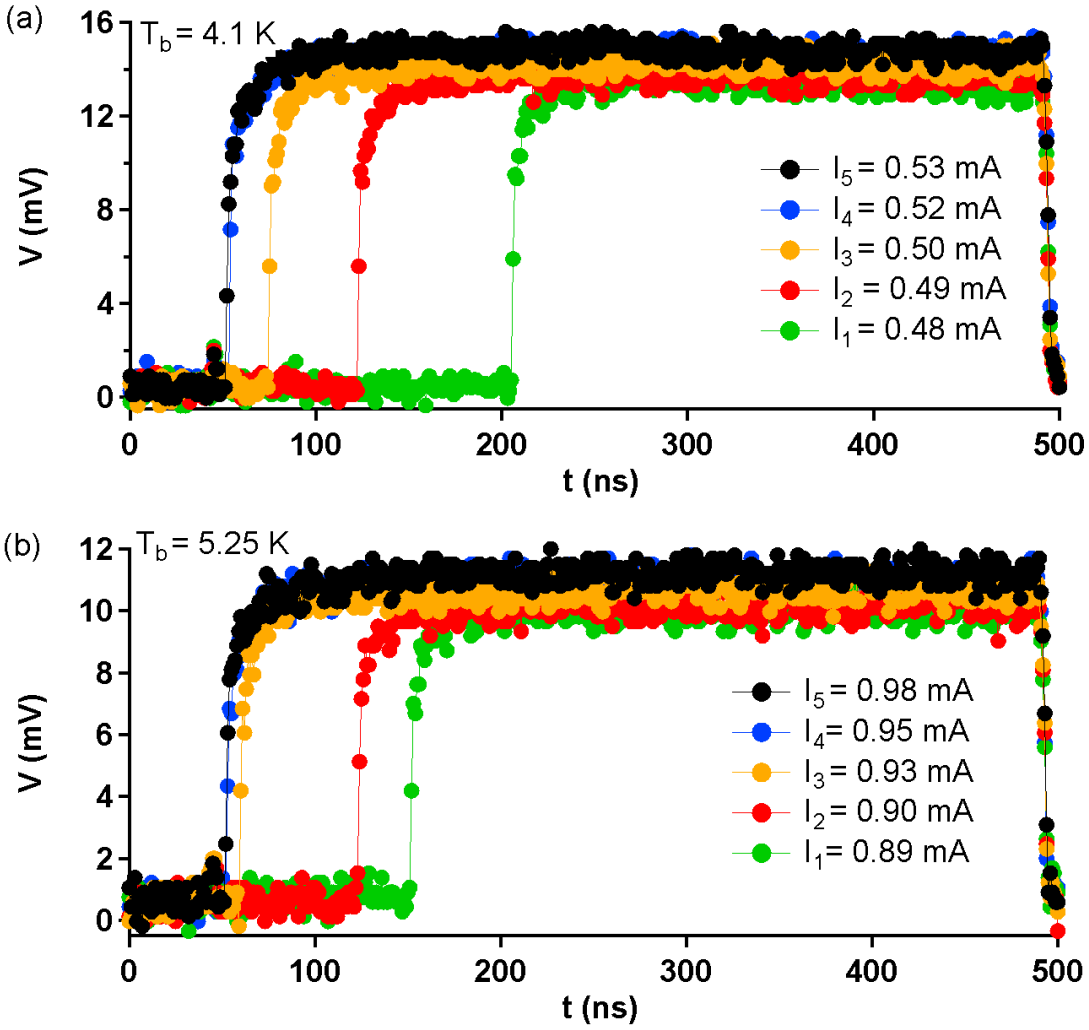

Figure 5.4: Voltage response plotted as a function of time at different temperature and different current value above I_c for the NbTiN samples of 5 μm-wide, BK-NT5

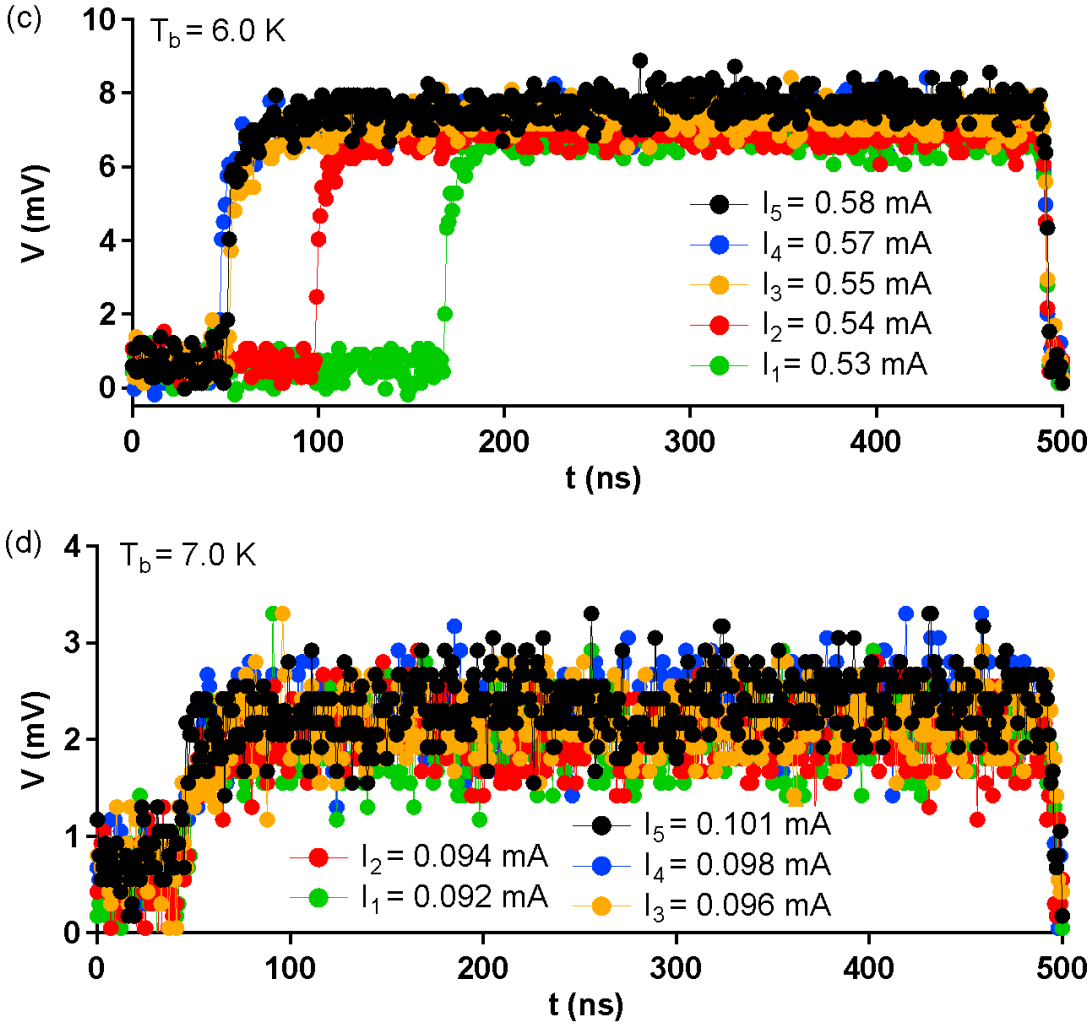

Figure 5.5: Voltage response plotted as a function of time at different temperature and different current value above I_c for the NbTiN samples of 5 μm-wide, BK-NT5

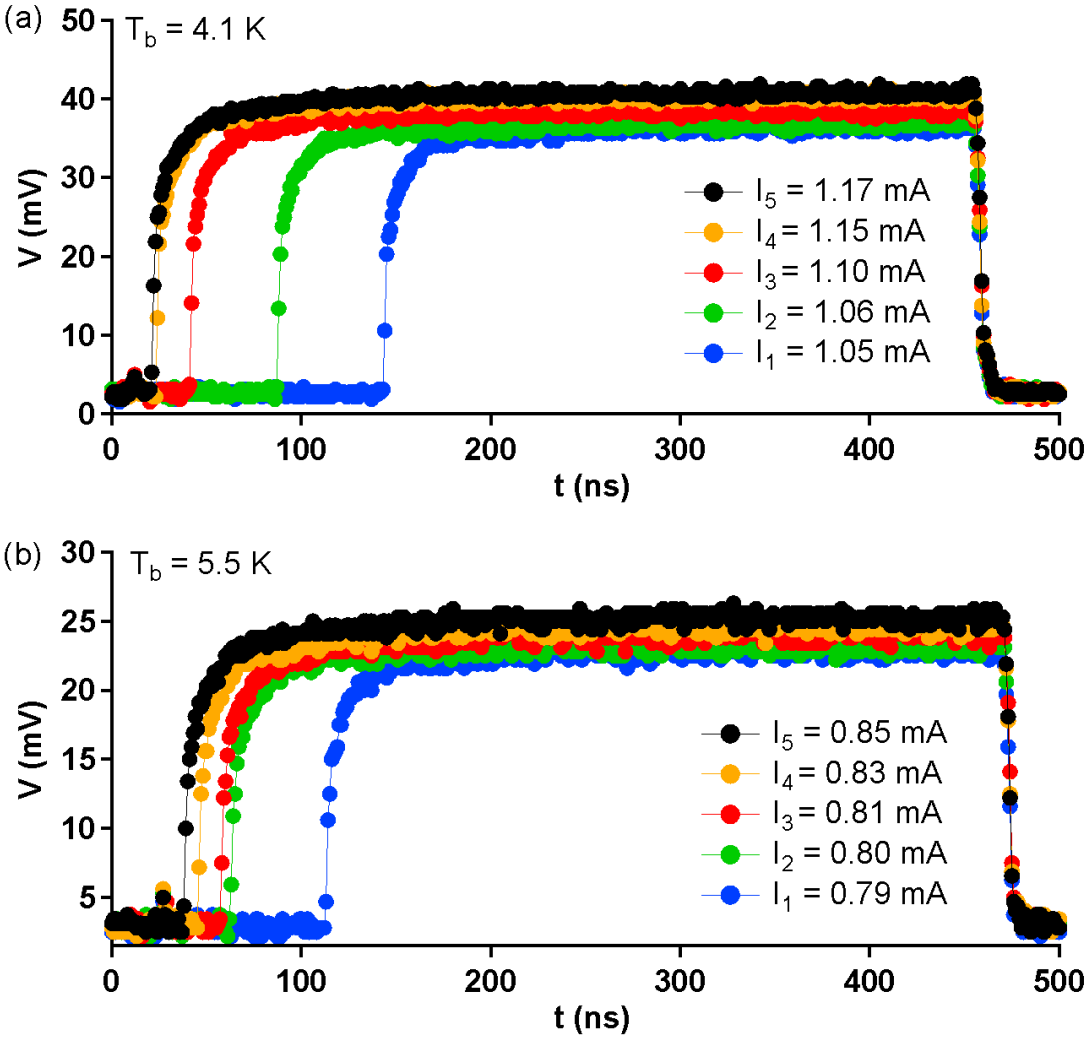

Figure 5.6: Voltage response plotted as a function of time at different temperature and different current value above I_c for the NbTiN samples of 10 μm-wide, BK-NT10

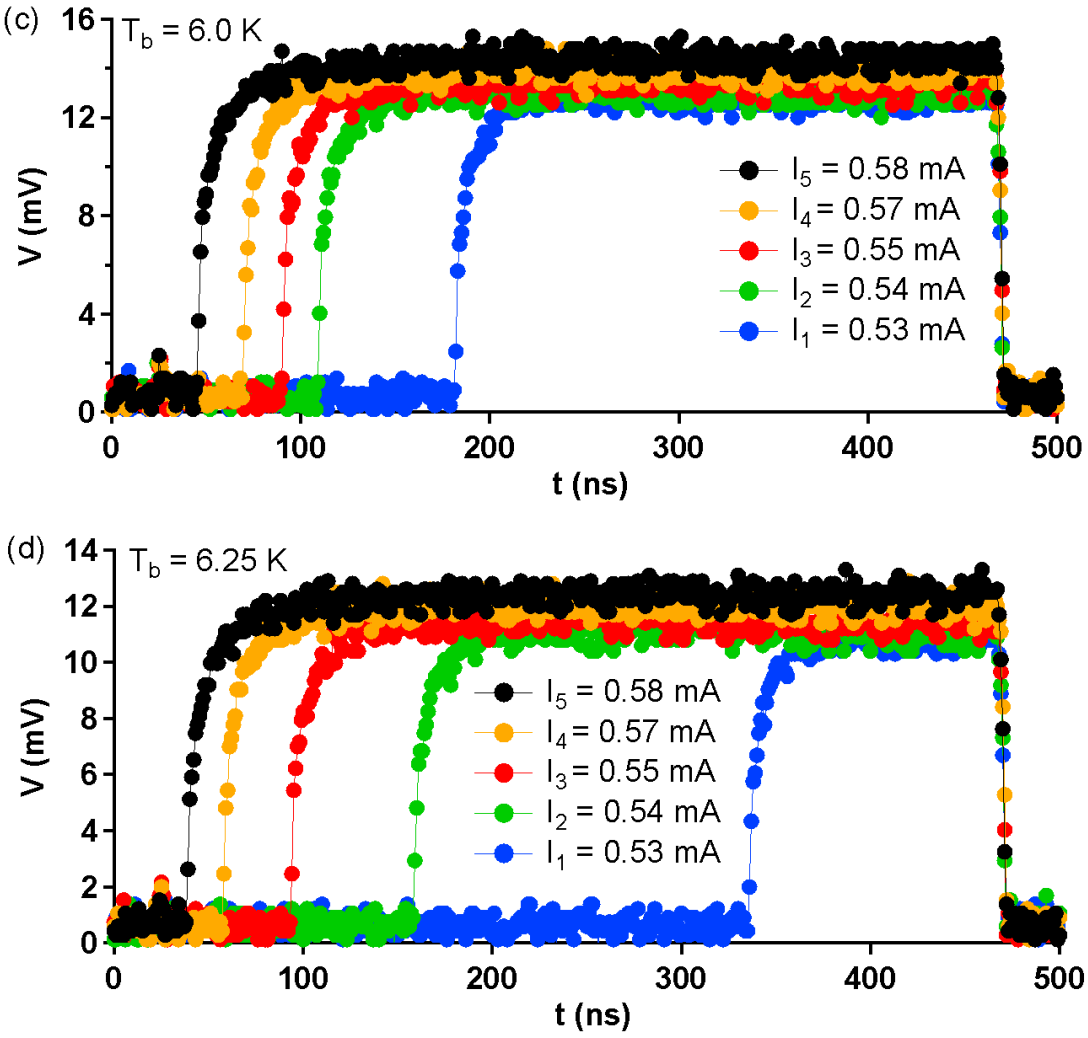

Figure 5.7: Voltage response plotted as a function of time at different temperature and different current value above I_c for the NbTiN samples of 10 μm-wide, BK-NT10

Appendix C

MORE RESULTS AND DATA ANALYSIS

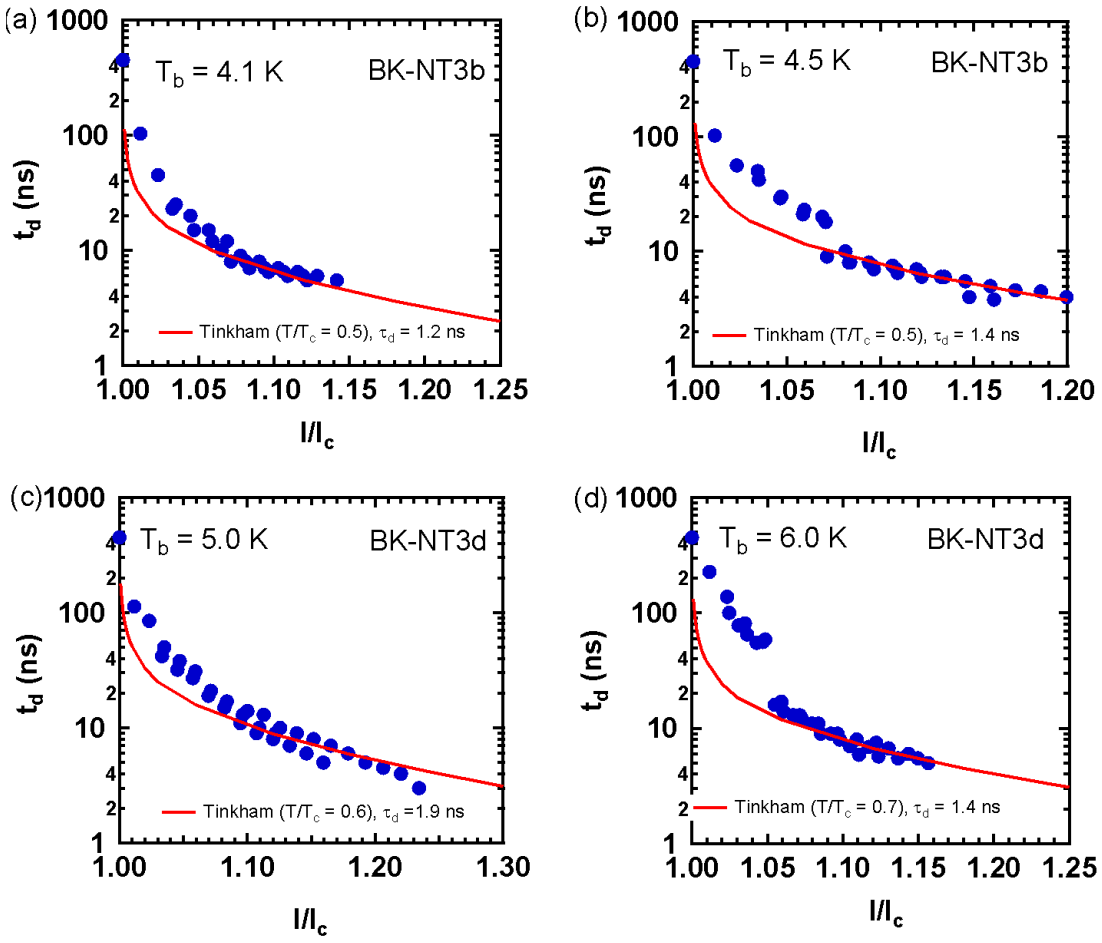

Figure 5.8: Delay time t_d as a function of I/I_c at different T_b in sample BK-NT3. The t_d axis is in logarithm scale. The solid curve is the Tinkham's fitting obtain from Eq. (4.2)

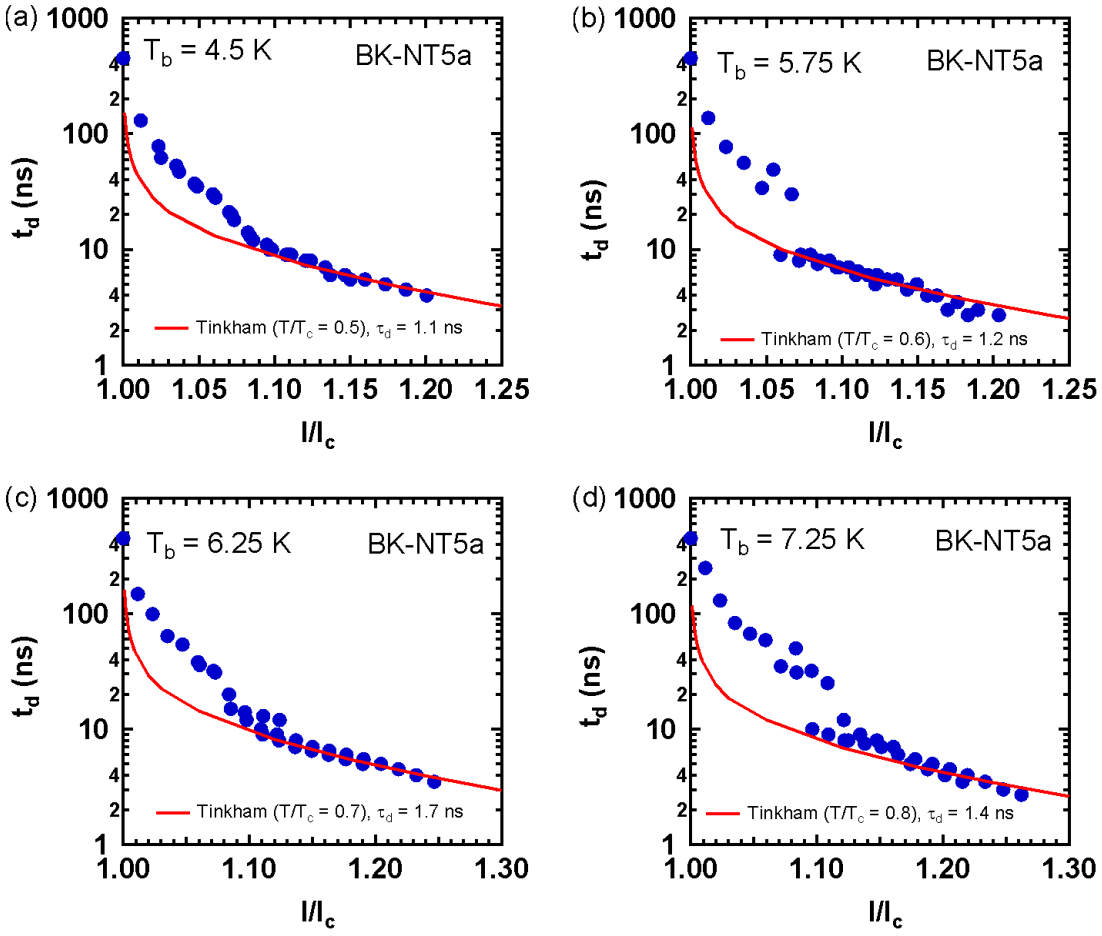

Figure 5.9: Delay time t_d as a function of I/I_c at different T_b in sample BK-NT5. The t_d axis is in logarithm scale. The solid curve is the Tinkham's fitting obtain from Eq. (4.2)

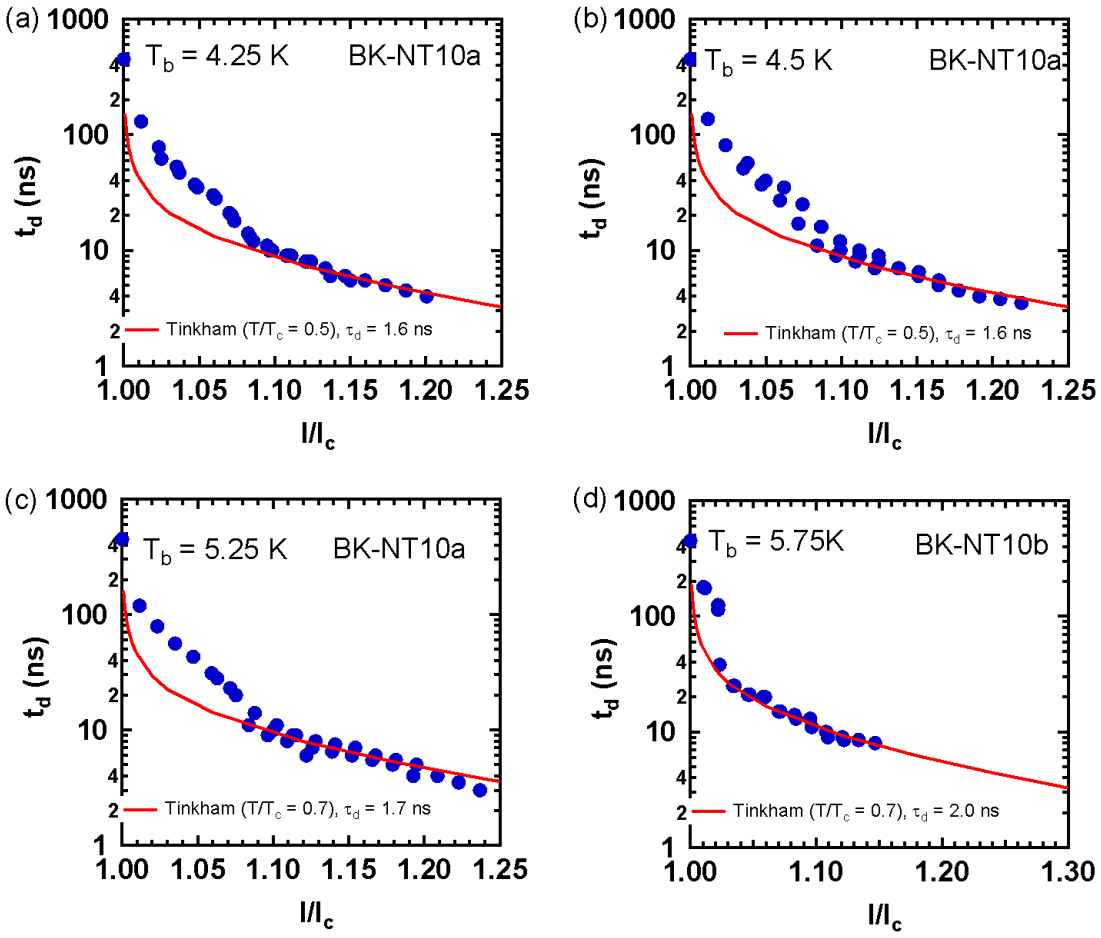

Figure 5.10: Delay time t_d as a function of I/I_c at different T_b in sample BK-NT10. The t_d axis is in logarithm scale. The solid curve is the Tinkham's fitting obtain from Eq. (4.2)

REFERENCES

[1] M. Tinkham, "Introduction to superconductivity," 1996.

[2] C. M. Natarajan, M. G. Tanner, and R. H. Hadfield, "Superconducting nanowire single-photon detectors: physics and applications," *Superconductor Science and Technology*, vol. 25, no. 6, p. 063001, 2012.

[3] D. v. Delft and P. Kes, "The discovery of superconductivity," *Physics Today*, vol. 63, no. 9, pp. 38–43, Sep. 2010. [Online]. Available: http://scitation.aip.org/content/aip/magazine/physicstoday/article 63/9/10.1063

[4] A. Taylor, *Superconductivity. Taylor*, ser. Wykeham science series. Wykeham, 1970.

[5] J. M. i. Tokyo, "Japan's maglev train breaks world speed record with 600km/h test run." [Online]. Available: http://www.theguardian.com/world/2015/apr/21/japans-maglev-train-notches-up-new-world-speed-record-in-test-run

[6] V. V. Shmidt, "The Critical Current in Superconducting Films," *Soviet Journal of Experimental and Theoretical Physics*, vol. 30, p. 1137, 1969. [Online]. Available: http://adsabs.harvard.edu/abs/1969JETP...30.1137S

[7] C. J. Olsen, C. Reichhardt, and F. Nori, "Nonequilibrium dynamics phase diagram for vortex lattices." *Phys. Rev. Lett.*, vol. 81, pp. 3757–3760, 1998. [Online]. Available: http://dx.doi.org/10.1103/PhysRevLett.81.3757

[8] J. Bardeen and M. J. Stephen, "Theory of the Motion of Vortices in Superconductors," *Phys. Rev.*, vol. 140, no. 4A, pp. A1197–A1207, Nov. 1965. [Online]. Available: http://link.aps.org/doi/10.1103/PhysRev.140.A1197

[9] I. Aranson, B. Y. Shapiro, and V. Vinokur, "Nucleation and Growth of the Normal Phase in Thin Superconducting Strips," *Phys. Rev. Lett.*, vol. 76, no. 1, pp. 142–145, Jan. 1996.

[10] J. Wolter, P. M. T. M. van Attekum, R. E. Horstman, and M. C. H. M. Wouters, "Temperature dependent time delay of the voltage response to supercritical current pulses in superconducting aluminium," *Solid State Communications*, vol. 40, no. 4, pp. 433–435, Oct. 1981. [Online]. Available: http://www.sciencedirect.com/science/article/pii/0038109881908553

[11] L. R. Testardi, "Destruction of Superconductivity by Laser Light," *Phys. Rev. B*, vol. 4, no. 7, pp. 2189–2196, Oct. 1971. [Online]. Available: http://link.aps.org/doi/10.1103/PhysRevB.4.2189

[12] V. F. Gantmakher, M. V. Golubkov, V. T. Dolgopolov, G. E. Tsydynzhapov, and A. A. Shashkin, "Destruction of localized electron pairs above the magnetic-field-driven superconductor-insulator transition in amorphous In-O films," *Journal of Experimental and Theoretical Physics Letters*, vol. 68, no. 4, pp. 363–369, 1998. [Online]. Available: http://link.springer.com/article/10.1134/1.567874

[13] J. Bardeen, L. N. Cooper, and J. R. Schrieffer, "Theory of Superconductivity," *Phys. Rev.*, vol. 108, no. 5, pp. 1175–1204, Dec. 1957. [Online]. Available: http://link.aps.org/doi/10.1103/PhysRev.108.1175

[14] J. G. Bednorz and K. A. MÃ$\frac{1}{4}$ller, "Possible highT c superconductivity in the Baâˆ'Laâˆ'Cuâˆ'O system," *Z. Physik B - Condensed Matter*, vol. 64, no. 2, pp. 189–193, Jun. 1986. [Online]. Available: http://link.springer.com/article/10.1007/BF01303701

[15] H. Liu, Z. Ye, W. Wu, and K. Rathnayaka, "Localized phase-slip centers in proximity-induced long superconducting nanowires," *Journal of Applied Physics*, vol. 105, no. 7, pp. 07E305–07E305, 2009.

[16] Y. B. Kim, C. F. Hempstead, and A. R. Strnad, "Flux-Flow Resistance in Type-II Superconductors," *Phys. Rev.*, vol. 139, no. 4A, pp. A1163–A1172, Aug. 1965. [Online]. Available: http://link.aps.org/doi/10.1103/PhysRev.139.A1163

[17] K. Harrabi, "Resistive states created in superconducting NbTiN filaments by an electrical current pulse," *AIP Advances*, vol. 5, no. 3, p. 037102, Mar. 2015. [Online]. Available: http://scitation.aip.org/content/aip/journal/adva/5/3/10.1063/1.4914103

[18] S. Miki, M. Takeda, M. Fujiwara, M. Sasaki, A. Otomo, and Z. Wang, "Superconducting NbTiN Nanowire Single Photon Detectors with Low Kinetic Inductance," *Appl. Phys. Express*, vol. 2, no. 7, p. 075002, Jul. 2009. [Online]. Available: http://iopscience.iop.org/1882-0786/2/7/075002

[19] A. J. Annunziata, O. Quaranta, D. F. Santavicca, A. Casaburi, L. Frunzio, M. Ejrnaes, M. J. Rooks, R. Cristiano, S. Pagano, A. Frydman, and D. E. Prober, "Reset dynamics and latching in niobium superconducting nanowire single-photon detectors," *Journal of Applied Physics*, vol. 108, no. 8, p. 084507, Oct. 2010. [Online]. Available: http://scitation.aip.org/content/aip/journal/jap/108/8/10.1063/1.3498809

[20] J. D. Meyer, "Spannungsstufen in denU (T)-Ãœbergangskurven undU (I)-Kennlinien stromtragender Zinn-Whisker," *Appl. Phys.*, vol. 2, no. 6, pp. 303–320, Dec. 1973. [Online]. Available: http://link.springer.com/article/10.1007/BF00896936

[21] A. K. Elmurodov, F. M. Peeters, D. Y. Vodolazov, S. Michotte, S. Adam, F. d. M. de Horne, L. Piraux, D. Lucot, and D. Mailly, "Phase-slip phenomena in NbN superconducting nanowires with leads," *Phys. Rev. B*, vol. 78, no. 21, p. 214519, Dec. 2008. [Online]. Available: http://link.aps.org/doi/10.1103/PhysRevB.78.214519

[22] W. J. Skocpol, M. R. Beasley, and M. Tinkham, "Phase-slip centers and nonequilibrium processes in superconducting tin microbridges," *J Low Temp Phys*, vol. 16, no. 1-2, pp. 145–167, Jul. 1974. [Online]. Available: http://link.springer.com/article/10.1007/BF00655865

[23] K. Harrabi, "Hotspot Temperatures Reached in Current-Driven Superconducting Niobium Filaments," *J Supercond Nov Magn*, vol. 26, no. 5, pp. 1865–1868, Jan. 2013. [Online]. Available: http://link.springer.com/article/10.1007/s10948-012-2042-y

[24] ——, "Temperature dependence of the film cooling time deduced from the time of nucleation of a dissipative zone in a superconducting YBa lt;sub>2 lt;/sub>Cu lt;sub>3 lt;/sub>O lt;sub>7 lt;/sub> Filament," *IEEE Transactions on Applied Superconductivity*, vol. PP, no. 99, pp. 1–1, 2016.

[25] F.-R. Ladan, K. Harrabi, M. Rosticher, P. Mathieu, J.-P. Maneval, and C. Villard, "Current-Temperature Diagram of Resistive States in Long Superconducting Niobium Filaments," *J Low Temp Phys*, vol. 153, no. 3-4, pp. 103–122, Oct. 2008. [Online]. Available: http://link.springer.com/article/10.1007/s10909-008-9821-7

[26] J. Maneval, K. Harrabi, F. Chibane, M. Rosticher, F. Ladan, and P. Mathieu, "Temperature Profile of Hotspots in Narrow Current-Biased Superconducting Strips," *Applied Superconductivity, IEEE Transactions on*, vol. 23, no. 3, pp. 2 200 604–2 200 604, 2013.

[27] K. Harrabi, F.-R. Ladan, V. D. Lam, J.-P. Maneval, J.-F. Hamet, J.-C. VillÃ©gier, and R. W. Bland, "Current-Temperature Diagram of Resistive States in Long Superconducting YBa2cu3o7 Strips," *J Low Temp Phys*, vol. 157, no. 1-2, pp. 36–56, Sep. 2009. [Online]. Available: http://link.springer.com/article/10.1007/s10909-009-9930-y

[28] T. Peterson, I. Maartense, and R. Biggers, "Self-heating hotspot effects in HTS thin films," *Applied Superconductivity, IEEE Transactions on*, vol. 5, no. 2, pp. 1436–1439, 1995.

[29] P. L. Richards, "Bolometers for infrared and millimeter waves," *Journal of Applied Physics*, vol. 76, no. 1, pp. 1–24, Jul. 1994. [Online]. Available: http://scitation.aip.org/content/aip/journal/jap/76/1/10.1063/1.357128

[30] J. Clarke, G. I. Hoffer, P. L. Richards, and N.-H. Yeh, "Superconductive bolometers for submillimeter wavelengths," *Journal of Applied Physics*, vol. 48, no. 12, pp. 4865–4879, Dec. 1977. [Online]. Available: http://scitation.aip.org/content/aip/journal/jap/48/12/10.1063/1.323612

[31] K. Harrabi, A. F. Salem, K. Ziq, A. I. Mansour, S. Kunwar, J. P. Maneval, and G. Berdiyorov, "Characterization of the current-induced resistive spots in superconducting \hbox {YBa}_{2} \hbox {Cu}_{3} \hbox {O}_{7} strips," *Appl. Phys. A*, vol. 117, no. 4, pp. 2033–2036, Aug. 2014. [Online]. Available: http://link.springer.com/article/10.1007/s00339-014-8613-y

[32] J. Pals and J. Wolter, "Measurement of the order-parameter relaxation in superconducting Al-strips," *Physics Letters A*, vol. 70, no. 2, pp. 150–152, 1979.

[33] M. Tinkham, "Heating and Dynamic Enhancement in Metallic Weak Links," in *Nonequilibrium Superconductivity, Phonons, and Kapitza Boundaries*, ser. NATO Advanced Study Institutes Series, K. E. Gray, Ed. Springer US, 1981, no. 65, pp. 231–262. [Online]. Available: http://link.springer.com/chapter/10.1007/978-1-4684-3935-9$_8$

Vitae

Name: Fatai Olawale Bakare

Nationality: Nigerian

Date of Birth: 1st April, 1986

Email: *bakareOlawaleFatai27@gmail.com*

Permenant Address: 6 Ojora Street, Ajegunle-Apapa, Lagos, Nigeria

Education Background: Federal University of Technology, Minna, Nigeria. B.Tech. in Physics and Electronics (First-class honors). 2007 - 2012